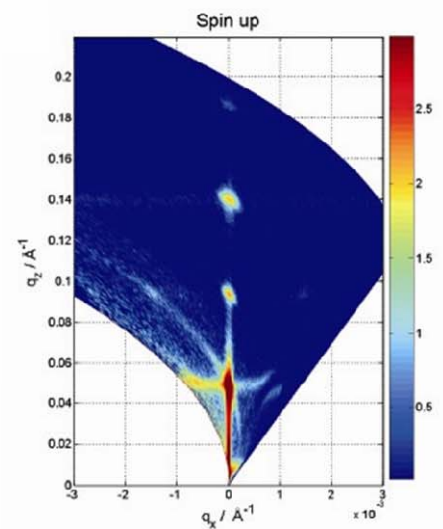
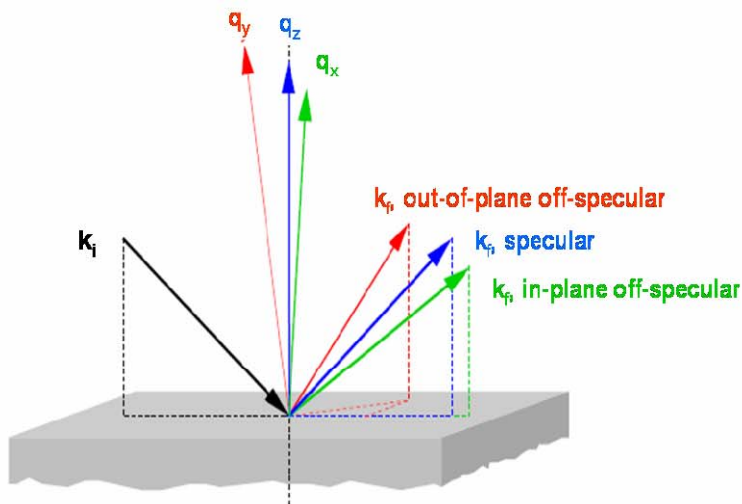


Reflectometry with X-rays and Neutrons



T. Gutberlet
LNS, PSI & ETHZ, Villigen

Outline

- **Basics of reflectometry**
 - **elastic scattering and scattering vector**
 - **specular and off-specular reflectivity**
 - **refractive index and Snell's law, critical angle**
 - **reflectivity of a bare interface, Fresnel reflectivity**
 - **penetration depth**
 - **reflectivity of a homogeneous slab, Kiessig fringes**
 - **reflectivity from a multilayer system, Parrat's recursive method**
 - **rough surfaces and interfaces**
 - **correlated surface roughness, diffuse scattering, coherence length**
 - **x-ray and neutron reflectometry, example of a Si/Pt monolayer**
 - **polarised neutron reflectometry**

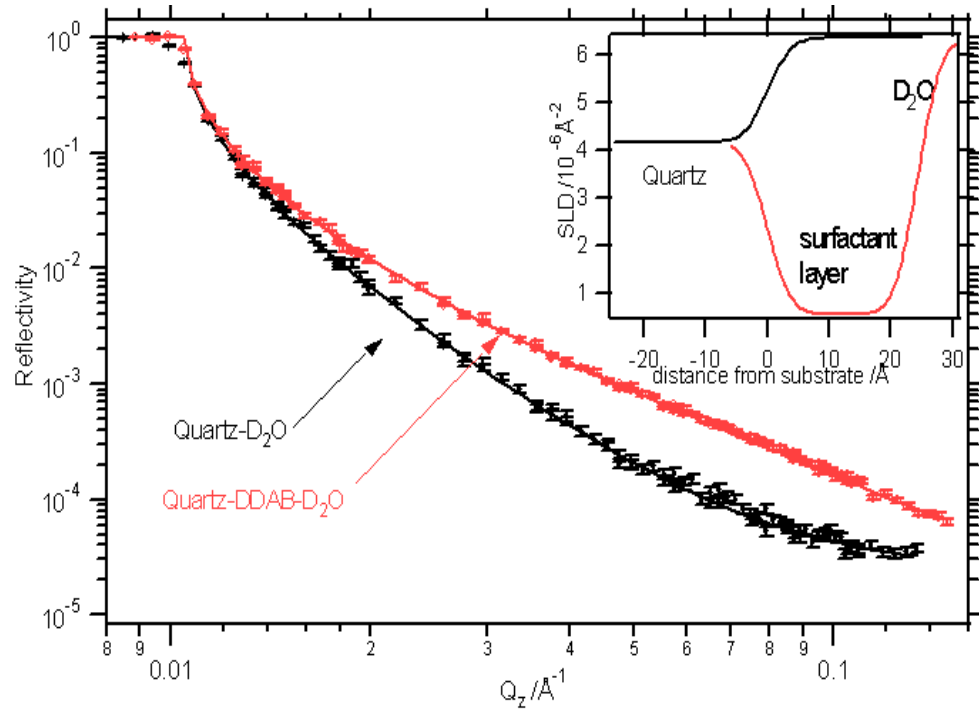
- **Reflectometry at solid/solid interfaces (neutron, x-ray)**
 - **intermetallic diffusion**
 - **magnetic multilayer systems**
 - **polarizing multilayer monochromators**

- **Reflectometry at solid/liquid interfaces (neutrons, x-ray)**
 - **biomembrane adsorption**
 - **polyelectrolyte cushions**

- **Reflectometry at liquid/liquid interfaces (x-ray, neutron)**

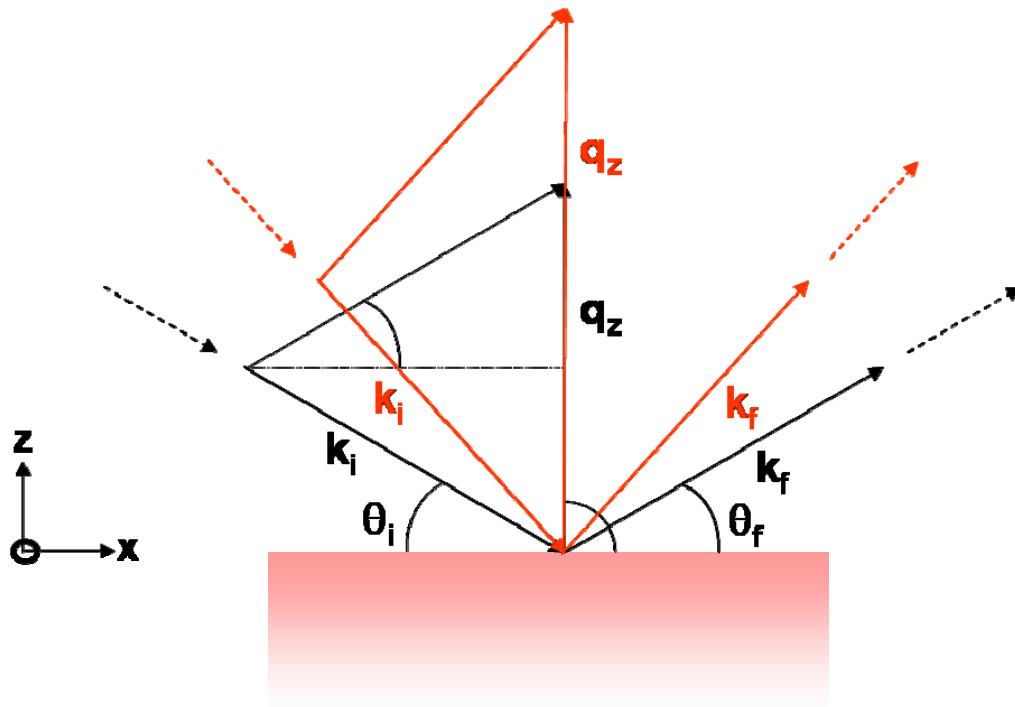
- **Reflectometry at air/liquid interfaces (x-ray, neutron)**
 - **Langmuir monolayers**
 - **foam films, black Newton films**

A simple reflectivity experiment



Data: G. Warr, A. Blom, Dept. of Chem., Univ. Sydney

Elastic scattering and scattering vector



The scattering of an incident wave is the same as the scattering of the scattered one and called **elastic scattering** when no energy is transferred in the scattering process. The momentum transfer in the elastic scattering event is given by

$$\begin{aligned} q_z &= k_i + k_f = k_f - k_i \\ &= (2\pi / \lambda \sin \theta_f) + (2\pi / \lambda \sin \theta_i) \\ &= 2\pi / \lambda (\sin \theta_f + \sin \theta_i) \end{aligned}$$

for $\theta_f = \theta_i$

$$q_z = 4\pi / \lambda \sin \theta$$

q_z is the wave vector transfer or **scattering vector** perpendicular to the direction of the scattered wave given by the incoming and outgoing wavevector k_i and k_f , respectively. The wavevector is given by the wavenumber

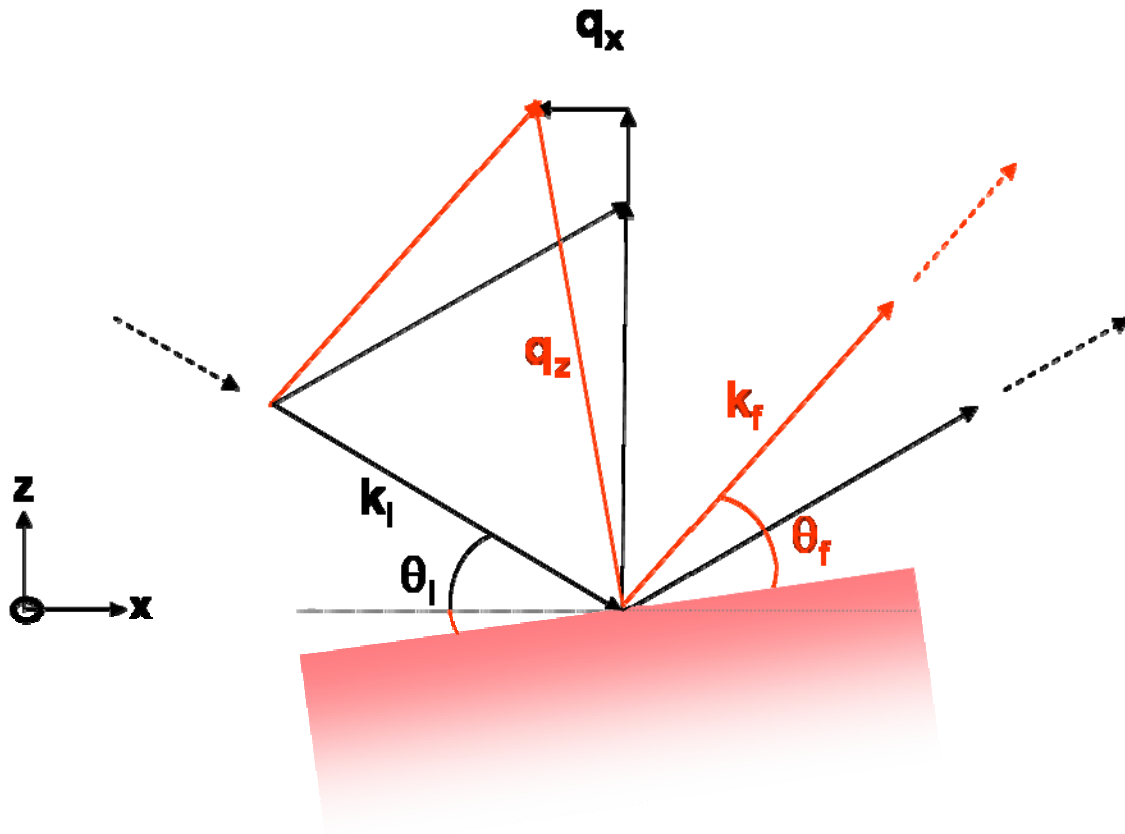
$$k = 2\pi / \lambda$$

describing the wave propagating along x over 2π with wavelength λ . The incident wave is a sine wave given by the real form as $\Psi_i = a_i \sin(k_i z)$ or in the complex form as $\Psi_i = a_i e^{ik_i z}$.

For equivalence of the incoming and outgoing scattering angle $\theta_f = \theta_i$ the reflected beam from the surface is called **specular**, and its intensity **specular reflectivity**.

Variation of the incoming scattering angle θ_i changes q_z . Experimentally this happens either changing θ_i of the incoming beam or by tilting the surface towards the incoming beam.

If by these changes $\theta_f = \theta_i$ is not kept equal, i.e. $\theta_f \neq \theta_i$ the wave vector transfer is split into a component along z and along x. The wavevector k_f then describes the scattered wave **off-specular in-plane** of the scattering plane, in our case the plane of the paper.



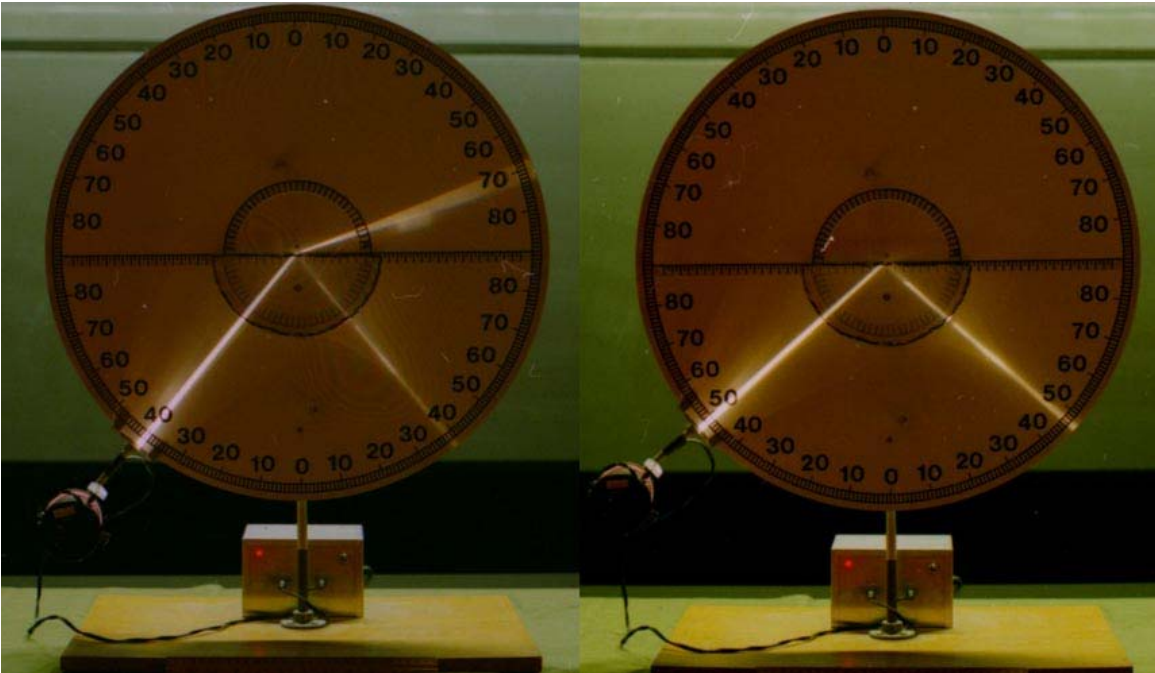
$$\begin{aligned}
 q_x &= k_i + k_r \\
 &= (2\pi / \lambda \cos \theta_r) - (2\pi / \lambda \cos \theta_i) \\
 &= 2\pi / \lambda (\cos \theta_r - \cos \theta_i)
 \end{aligned}$$

for $\theta_r = \theta_i$

$$q_x = 0$$

Refractive index and Snell's law

If the incoming wave is not totally scattered part of the beam is refracted into the medium below the interface.

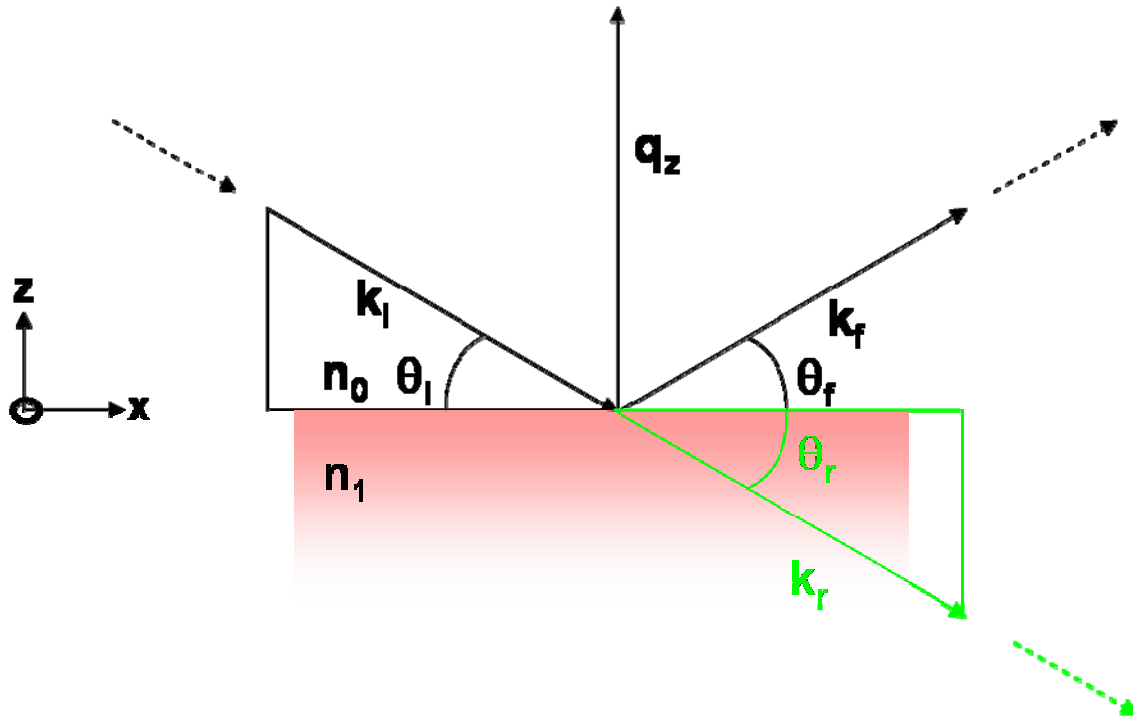


If the material at which the wave is refracted is of the same optical density as the material of the incoming wave the incoming and the refracted wave-vector are equal, i.e. there is no change of the wave velocity parallel to the surface and the ratio between k_i and k_f is unity

$$k_i / k_r = n = 1$$

$$a_i k \cos \theta = a_r k \cos \theta = a_i k n \cos \theta$$

Usually this is not the case and the refracted wavevector is different from the incoming wavevector by n , which is called refractive index.



$$\begin{aligned}
 n &= k_i / k_r \\
 &= \frac{a_i k \cos \theta_i + a_f k \cos \theta_f}{a_r k \cos \theta_r} \\
 &= \frac{(a_i + a_f) k \cos \theta}{a_r k \cos \theta}
 \end{aligned}$$

with the amplitude of the wavevector $a_i + a_f = a_r$

$$n = \frac{\cos \theta_i}{\cos \theta_r}$$

which is **Snell's law**. It follows

for $\theta_i = \theta_r$ follows $n = 1$

for $\theta_i > \theta_r$ follows $n < 1$

for $\theta_i < \theta_r$ follows $n > 1$

Usually the refractive index is smaller than 1 as the phase velocity of a refracted beam in a medium is higher as in vacuum. Thus n can be expressed as deviation from 1

$$n = \frac{\cos\theta}{\cos\theta} = 1 - \delta$$

Describing the relationship between the refractive index of a material and its scattering properties as either a phase shift in the refracted wave or as a superposition of spherical waves the total wave is given either as

$$\Psi_{tot} = \Psi_0[1 + i(n-1)k\Delta k]$$

or as

$$\Psi_{tot} = \Psi_0\left[1 - \frac{i(2\pi\rho b\Delta)}{k}\right]$$

This leads to the following relationship with n to express δ

$$\Psi_0[1 + i(n-1)k\Delta] = \Psi_0\left[1 - \frac{i(2\pi\rho b\Delta)}{k}\right]$$

$$i(n-1)k\Delta = \frac{-i(2\pi\rho b\Delta)}{k}$$

$$-n + 1 = \frac{2\pi\rho b\Delta}{k^2}$$

$$n = 1 - \frac{2\pi}{k_i^2} \rho b = 1 - \delta$$

Here Δ is the thickness of the material, ρb is the scattering length density with the coherent scattering length ρ and the number density b .

For $\theta_r = 0$, the remaining angle θ is the **critical angle of total reflection** θ_c

$$\cos \theta_i = \cos \theta_c = 1 - \delta$$

$$1 - \frac{\theta_c^2}{2!} + \dots = 1 - \delta$$

$$\theta_c = \sqrt{2\delta}$$

$$= \sqrt{2 \frac{2\pi}{k_i^2} \rho b}$$

$$= \frac{2}{k_i} \sqrt{\pi \rho b}$$

The corresponding **critical wave vector** q_c is

$$q_c = 2k\theta_c = 2k\sqrt{2\delta} = 4\sqrt{\pi\rho b}$$

Reflectivity of a bare interface

The reflectivity intensity R is defined as the product of the amplitude reflectivity r with its conjugate complex r^* expressed by the ratio of incident and outgoing amplitude a_i / a_f

$$R = |a_i / a_f|^2 = r^* r$$

The incident, outgoing and refracted waves

$\Psi_i = a_i e^{ik_i r}$, $\Psi_f = a_f e^{ik_f r}$, $\Psi_r = a_r e^{ik_r r}$ show for the amplitudes at $z = 0$

$$a_i + a_f = a_r$$

$$a_i k_i + a_f k_f = a_r k_r$$

with $k = |k_i| = |k_f|$ and $nk = k_r$ follows

$$a_r n k \cos \theta_r = a_i k \cos \theta_i + a_f k \cos \theta_f$$

$$n a_r k \sin \theta_r = (a_i - a_f) k \sin \theta_i$$

$$n = \frac{(a_i - a_f) \sin \theta_i}{(a_i + a_f) \sin \theta_r}$$

$$n \frac{\sin \theta_r}{\sin \theta_i} = \frac{(a_i - a_f)}{(a_i + a_f)} \approx \frac{\theta_f}{\theta_i}$$

$$r \equiv \frac{a_r}{a_i} = \frac{\theta_i - \theta_f}{\theta_i + \theta_f}$$

which is the **Fresnel equation of reflectivity**, and

$$t \equiv \frac{a_r}{a_i} = \frac{2\theta_i}{\theta_i + \theta_f}$$

which is the Fresnel equation of transmittivity. The resulting reflectivity intensity R then is

$$R = r * r = \left(\frac{\theta_i - \theta_f}{\theta_i + \theta_f} \right)^2$$

With $q_z = 4\pi / \lambda \sin \theta_f = 2k \sin \theta_f \approx 2k \theta_f$ it can be written

$$R = r * r = \left(\frac{q_i - q_r}{q_i + q_r} \right)^2$$

Using $q_r^2 = q_i^2 - q_c^2$

$$\begin{aligned}
R = r * r &= \left(\frac{q_i - \sqrt{q_i^2 - q_c^2}}{q_i + \sqrt{q_i^2 - q_c^2}} \right)^2 \\
&= \left(\frac{(1 - \sqrt{q_i^2 - q_c^2}) / q_i}{(1 + \sqrt{q_i^2 - q_c^2}) / q_i} \right)^2 \\
&= \left(\frac{(1 - \sqrt{1 - (q_c / q_i)^2})}{(1 + \sqrt{1 - (q_c / q_i)^2})} \right)^2
\end{aligned}$$

For $q_i^2 > q_c^2$ the reflectivity intensity leads to

$$R(q) \approx \left(\frac{q_c}{q_i} \right)^4$$

Penetration depth

A wave propagating in a medium has its amplitude according to

$$e^{inkz} = e^{i(1-\delta)kz} e^{-\beta kz}$$

where $e^{i(1-\delta)kz}$ is the dispersion of the wave in the material and $e^{-\beta kz}$ the adsorption of the wave in the medium. Then the refractive index is given by

$$n = 1 - \delta - i\beta$$

with the real part giving the dispersion

$$\delta = \frac{2\pi}{k^2} \rho b = \frac{\lambda^2}{2\pi} \rho b$$

ρb is the scattering length density, and the imaginary part giving the adsorption

$$\beta = \frac{\lambda\mu}{4\pi} = \frac{\mu}{2k}$$

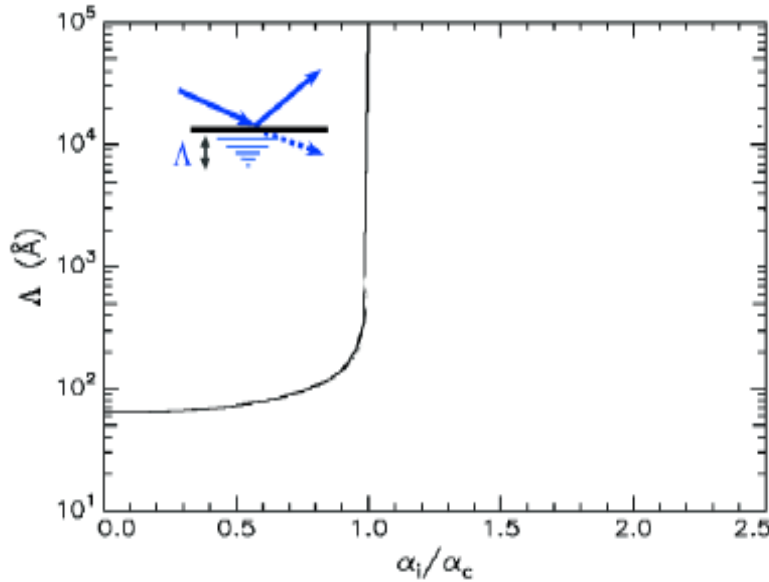
$$\mu = 2k\beta = \frac{4\pi}{\lambda}\beta$$

μ is the linear absorption coefficient. The penetration depth of the beam in the medium depends on the imaginary part of the refracted wave

$$a_r e^{i(k\theta_r)z} = a_r e^{ik \operatorname{Re}(\theta_r)z} e^{-k \operatorname{Im}(\theta_r)z}$$

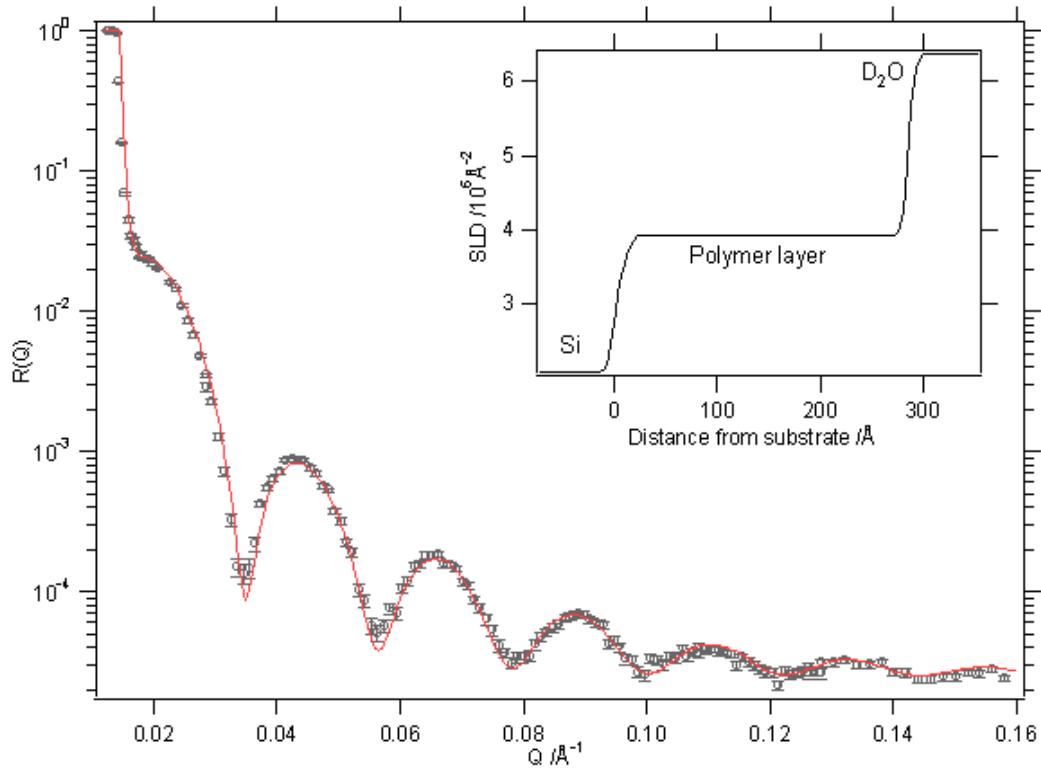
i.e. the penetration depth is

$$\Lambda = \frac{1}{2k \operatorname{Im}(\theta_r)} = \frac{1}{2k\beta} = \frac{1}{\mu} = -\frac{\lambda}{4\pi\beta}$$



Reflectivity of a homogenous slab

The reflectivity of a homogenous slab, i.e. the reflectivity from two interfaces separated by a slab of thickness d , is derived as follows. Each reflectivity and transmittivity component is added up taking into account the corresponding phase factor $p^2 = e^{iqd}$, with d thickness of slab.

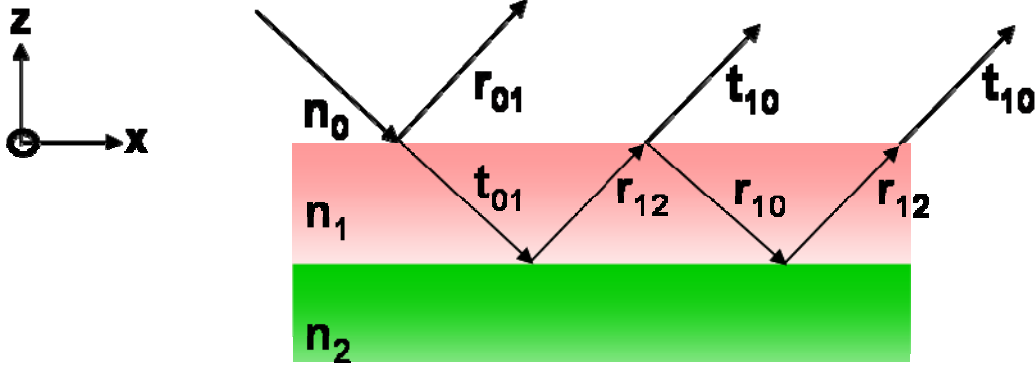


Data: P. Hartley et al., CSIRO Molecular Science, Clayton

$$\begin{aligned}
 r &= r_{01} + t_{01}r_{12}t_{10}p^2 + t_{01}r_{12}t_{10}p^2r_{10}r_{12}p^2 + \dots \\
 &= r_{01} + t_{01}r_{12}t_{10}p^2 \sum (r_{10}r_{12}p^2)^m \\
 &= r_{01} + t_{01}r_{12}t_{10}p^2 \frac{1}{1 - r_{10}r_{12}p^2}
 \end{aligned}$$

with $r_{01}^2 + t_{01}t_{10} = 1$ it follows $t_{01}t_{10} = 1 - r_{01}^2$ which leads to

$$r(1 - r_{10}r_{12}p^2) = r_{01}(1 - r_{10}r_{12}p^2) + (1 - r_{01}^2)r_{12}p^2$$



with $r_{01} = -r_{10}$

$$\begin{aligned}
 r &= r_{01} - r_{01}r_{10}r_{12}p^2 + r_{12}p^2 - r_{01}^2r_{12}p^2 \\
 &= r_{01} + r_{01}^2r_{12}p^2 + r_{12}p^2 - r_{01}^2r_{12}p^2 \\
 &= \frac{r_{01} + r_{12}p^2}{1 + r_{10}r_{12}p^2}
 \end{aligned}$$

The reflectivity intensity follows to

$$\begin{aligned}
 R &= r * r = \left(\frac{r_{01} + r_{12}p^2}{1 + r_{10}r_{12}p^2} \right)^2 \\
 &= \frac{r_{01}^2 + r_{12}^2 + 2r_{01}r_{12}e^{iqd}}{1 + r_{01}^2r_{12}^2 + 2r_{01}r_{12}e^{iqd}}
 \end{aligned}$$

with $e^{iqd} = \cos 2qd$

$$R = \frac{r_{01}^2 + r_{12}^2 + 2r_{01}r_{12} \cos qd}{1 + r_{01}^2r_{12}^2 + 2r_{01}r_{12} \cos qd}$$

The oscillations in the reflectivity profile result from the interference term in the above equation and depend on the thickness of the slab regarding the position and the difference in scattering contrasts between the respective interfaces regarding the amplitude. The oscillations are often called **Kiessig fringes**.

The expression for the reflectivity can be further reduced with $r_{01} = -r_{12}$ to

$$r = \frac{r_{01}(1 - p^2)}{(1 - r_{01}^2 p^2)}$$

For a thin slab $|r_{01}| \ll 1$ and

$$\begin{aligned} r_{slab} &= r_{01}(1 - p^2) \\ &= r_{01}(1 - e^{iq_1 d}) \end{aligned}$$

Using the Fresnel equation for r_{01} follows

$$\begin{aligned} r_{slab} &= \frac{(q_0 - q_1)}{(q_0 + q_1)}(1 - e^{iq_1 d}) \\ &= \frac{q_c^2}{4q_1^2}(1 - e^{iq_1 d}) \end{aligned}$$

and with $q_c = 2k\theta_c$ and $\theta_c = \frac{2}{k_i} \sqrt{\pi\rho b}$

$$\begin{aligned} r_{slab} &= -\frac{16\pi\rho b}{4q_1^2} e^{iq_1 d/2} (e^{iq_1 d/2} - e^{-iq_1 d/2}) \\ &= -i \frac{4\pi\rho b d}{q_1} e^{iq_1 d/2} \frac{\sin(q_1 d/2)}{q_1 d/2} \end{aligned}$$

Assuming $d \ll 1$ the equation can be reduced further to

$$r_{slab} = -i \frac{4\pi\rho b d}{q_1} = -i \frac{q_c^2}{4q_1} d$$

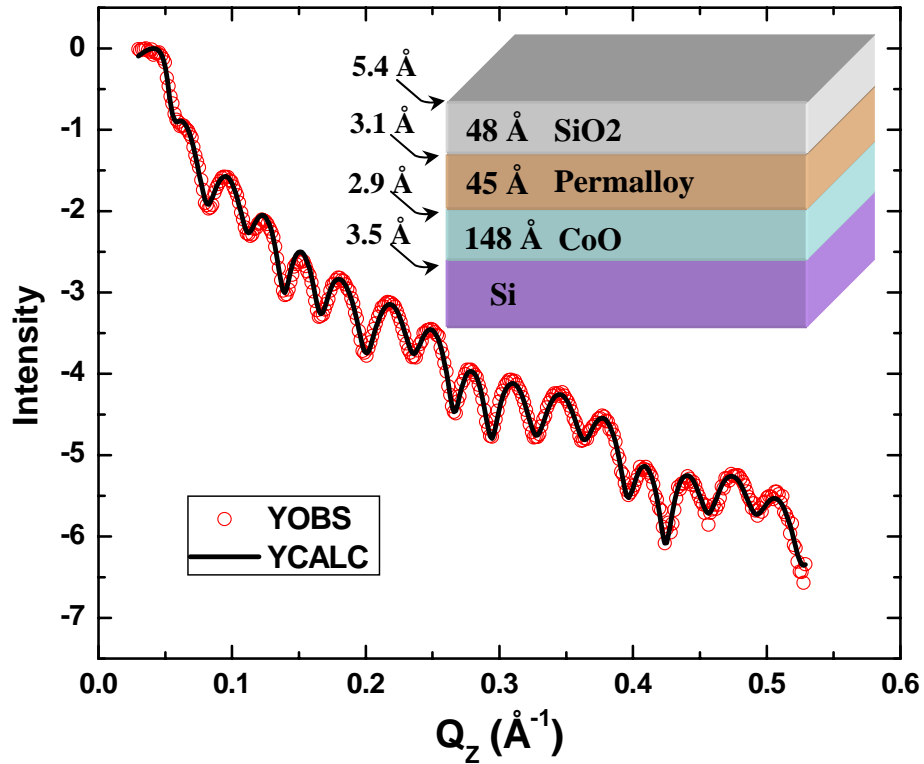
With $r(q) = \left(\frac{4\pi\rho b}{q_1^2} \right)^2$ the reflectivity intensity can be written as

$$R(q) = \left(\frac{q_c}{q_1} \right)^4 \left| \int \rho(z) e^{2iq_1 z} dz \right|^2$$

$$= R_F(q) \left| \int \rho(z) e^{2iq_1 z} dz \right|^2$$

Where $\rho(z)$ is the scattering length density profile along z . In case of sharp interfaces a step function results. $R_F(q)$ is the intensity of the Fresnel reflectivity and the above equation is termed Master formula in the literature.

Reflectivity from a multilayer system



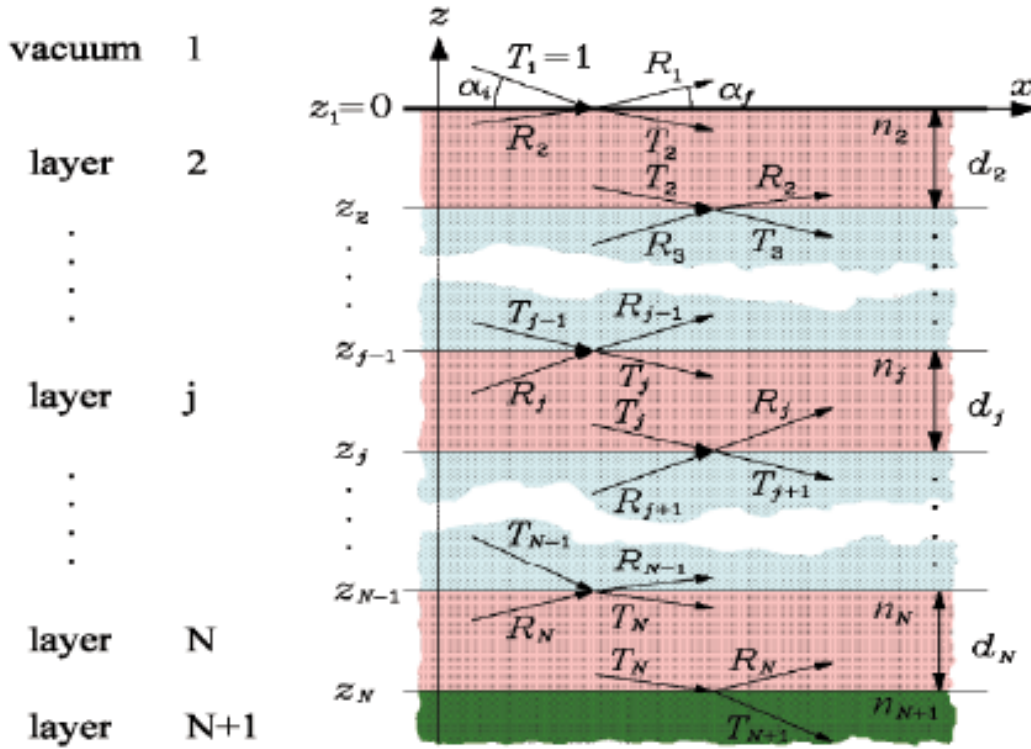
Specular reflection from multilayers is obtained by the reflectivity of each interface according to the Fresnel relation

$$r_{j,j+1} = \frac{\theta - \theta_{j,j+1}}{\theta + \theta_{j,j+1}}$$

which leads recursively for all interfaces to

$$r_{j,j+1} = \frac{r_{j,j+1} + r_{j+1} e^{2iq_{j+1}d_j}}{1 + r_{j,j+1}r_{j+1} e^{2iq_{j+1}d_j}}$$

This method is called **Parrat's recursive method**, who derived this method in 1954, or optical matrix formalism of stratified media.



A similar expression is obtained within the kinematical approximation of the reflectivity from ν layers comprising a multilayer.

$$\begin{aligned} r_\nu(\zeta) &= \sum (\zeta) e^{i2\pi\zeta\nu} e^{-\beta\nu} \\ &= r_1(\zeta) \frac{1 - e^{i2\pi\zeta\nu} e^{-\beta\nu}}{1 - e^{i2\pi\zeta} e^{-\beta}} \end{aligned}$$

In the kinematical approximation multiple reflections and refraction are assumed to be small and can be neglected. This is called Born approximation. It is valid at angles well away from the critical angle.

If the system has repeating subunits with equal distance d the reflected intensity superimposes giving rise to Bragg peaks in the reflectivity pattern which obey Bragg's law $n\lambda = 2d \sin \theta$.

Rough surfaces and interfaces

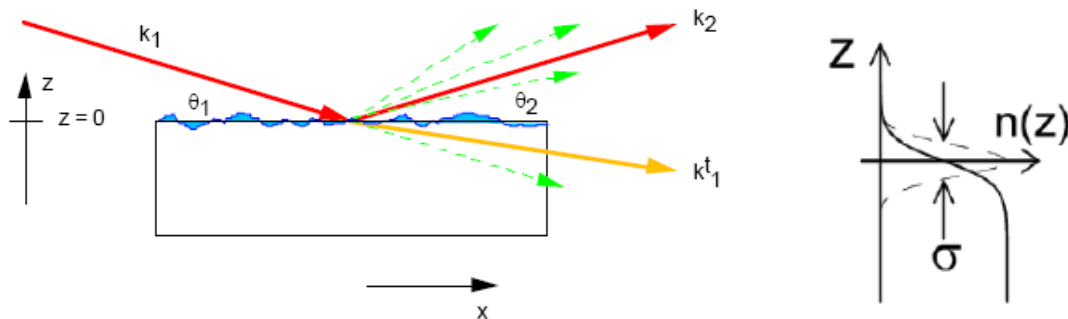
Usually an interface is not ideally sharp and the reflectivity is damped by diffuse scattering due to surface roughness expressed as

$$R(q) = R_F(q)e^{-q^2\sigma^2}$$

The damping of the diffuse scattering is the Fourier transform of the derivative of the error function $f(z) = \text{erf}\left(\frac{z}{\sqrt{2}\sigma}\right)$, which is a Gaussian.

The error function describes the density distribution at the rough interface. Basically the ideally sharp density profile is convoluted with a Gaussian smoothing function or Debye-Waller factor. σ is a measure of the width of the interface roughness given as rms roughness $\sigma = \sqrt{\langle h^2 \rangle}$.

Such a rough interface exhibits no correlation between the heights at different points of the surface. The scattering of the uncorrelated surface is confined to the specular direction.



Correlated surface roughness, diffuse scattering

The roughness of a surface can also be expressed as height fluctuations which can be described with a height-height correlation function.

$$C(\mathbf{r}) = \langle z(\mathbf{0})z(\mathbf{r}) \rangle = \sigma^2 e^{-(r/\xi)^2 h}$$

here ξ is the cut-off length in the xy-plane of the surface. For $R > \xi$ the interface is smooth, for the $R < \xi$ interface is rough. The exponent h is known as Hurst parameter and is related to the fractal dimension of the surface with $h = 3 - D$ with $D = 2$ for smooth and $D = 3$ for rough surfaces, thus $0 < h < 1$. The scattering of the correlated surface roughness is off-specular, i.e. information about lateral correlation length can be obtained.

The scattering function is given by

$$S_{tot}(\mathbf{q}) = S_{spec}(\mathbf{q}) + S_{diff}(\mathbf{q})$$

with

$$S(\mathbf{q}) = \int \langle \rho(\mathbf{0})\rho(\mathbf{r}) \rangle e^{i\mathbf{q}\cdot\mathbf{r}} d^3\mathbf{r}$$

For the diffuse scattering one can develop the following expression

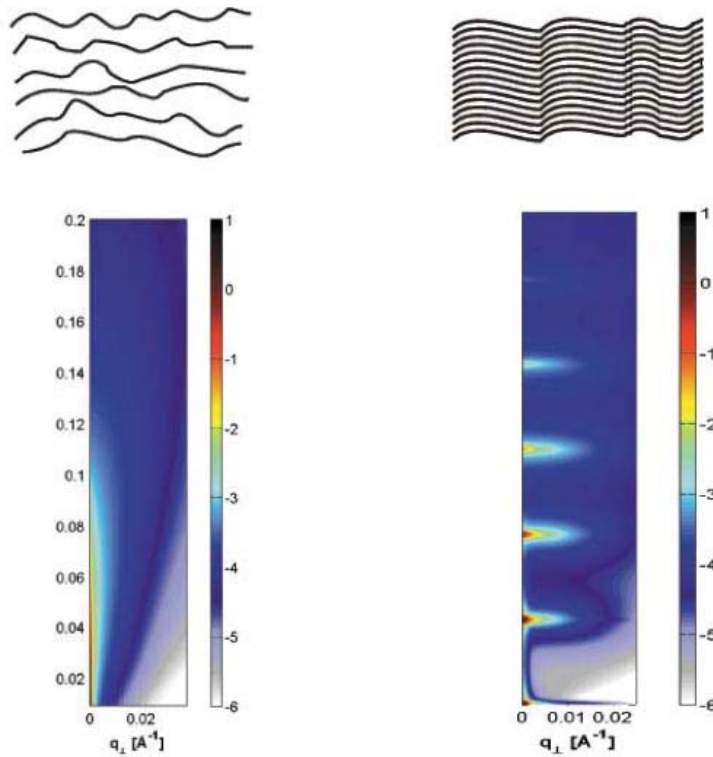
$$S_{diff}(\mathbf{q}) = \frac{1}{q_z^2 e^{-q_z^2 \sigma^2}} \int [e^{-q_z^2 C(\mathbf{r})} - 1] e^{i\mathbf{q}_x \cdot \mathbf{r}} d^2\mathbf{r}$$

here the wave vector transfer q_z as well as q_x and the height-height correlation function $C(\mathbf{r})$ are included.

For small distortions with $q_z \sigma < 1$

$$\begin{aligned} S_{diff}(\mathbf{q}) &= e^{-q_z^2 \sigma^2} \int C(\mathbf{r}) e^{i\mathbf{q}_x \cdot \mathbf{r}} d^2\mathbf{r} \\ &= e^{-q_z^2 \sigma^2} \times C(\mathbf{q}_x) \end{aligned}$$

Scattering of uncorrelated and correlated multilayers

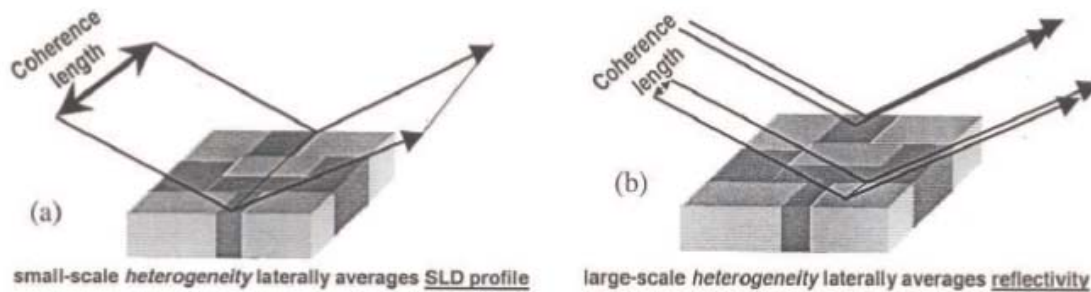


The scattering function is expressed as Fourier transform of the height-height correlation function damped by the roughness.

Coherence length

A beam impinging on a surface is in reality not perfect monochromatic nor does it propagate in a perfect defined direction. This means that a wave propagating in a direction with wavelength λ is accompanied by another wave in the same direction with $\lambda - \Delta\lambda$. At a certain point both waves are in phase and at a certain point away the two waves are completely out of phase. This difference in space between the two waves is called longitudinal coherence length L_L . The transverse coherence length L_T is defined for two waves of equal wavelength but slightly different propagation directions and the difference in space to be completely out of phase defines L_T .

The two coherence lengths together define the upper limit on the separation of two objects to distinguish them in a scattering experiment. E.g. for x-rays the coherence values are in the range of μm .



X-ray and neutron reflectometry

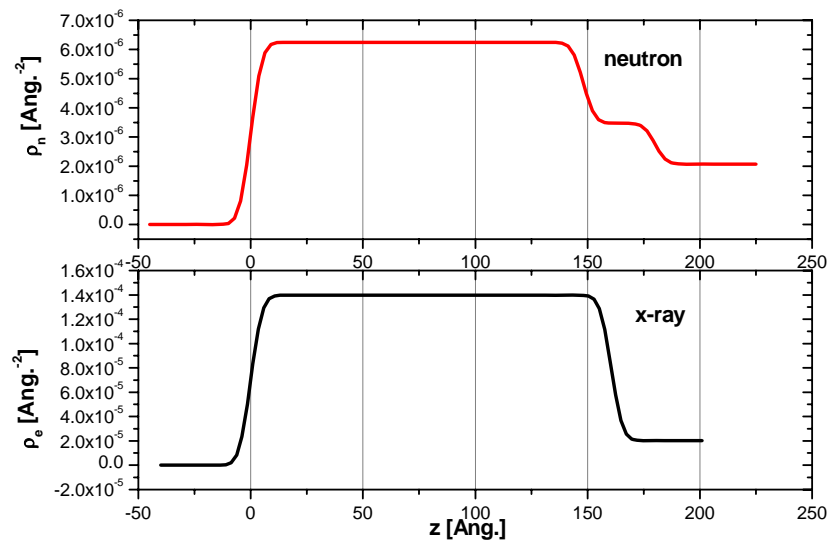
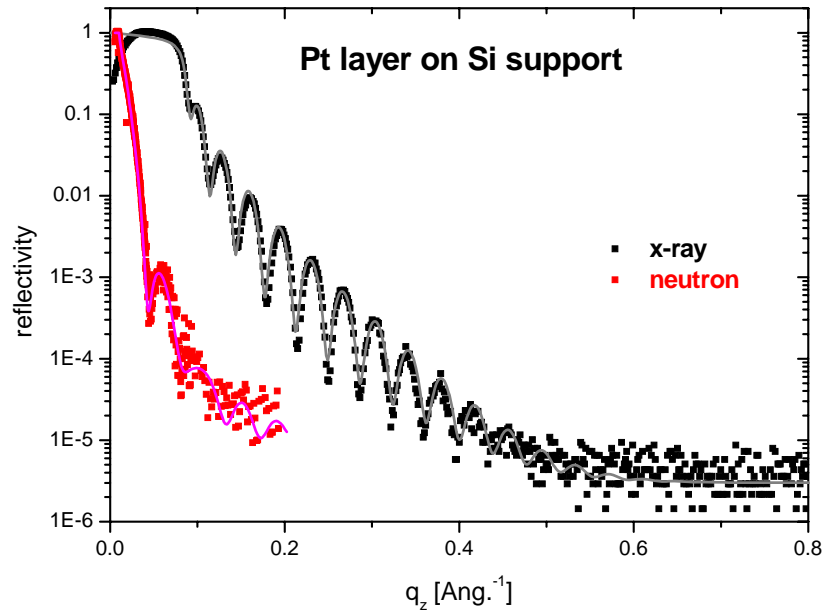
X-rays are an electromagnetic radiation. The photon energy is given by $E = h\nu = hc/\lambda = hck$, the charge is zero, the magnetic moment is zero and the spin is 1. X-rays show particle as well as wave properties.

Neutrons are an elementary particle with a mass of $m_n = 1.675 \cdot 10^{-27}$ kg, charge is zero, spin is $1/2$, the magnetic moment is $\mu_n = -1.913 \mu_n$, the nuclear magneton is $\mu_n = eh/4\pi m_p = 5.051 \cdot 10^{-27}$ JT⁻¹, the kinetic energy is $E = m_n v^2 / 2 = k_B T = (hk/2\pi)^2 / 2m_n$, with $k = 2\pi/\lambda$. It has particle as well as wave properties.

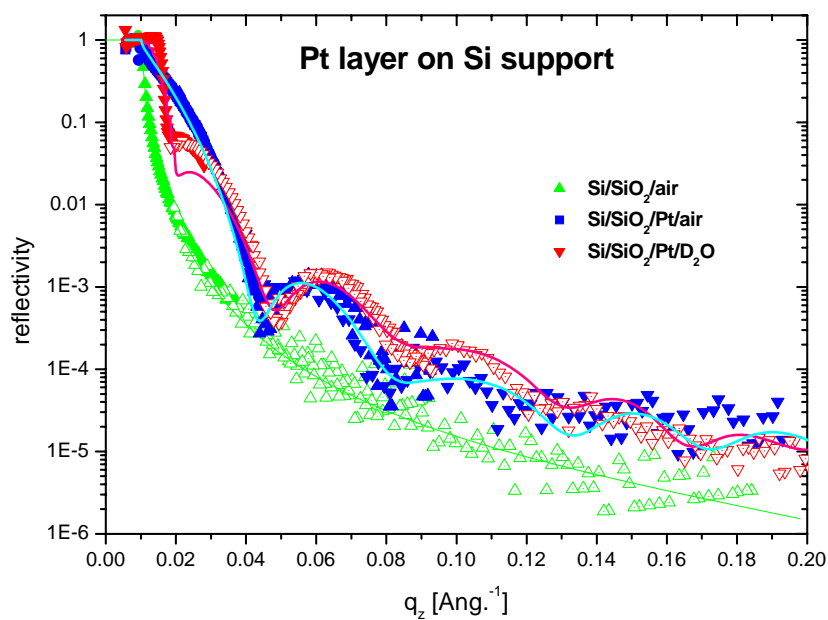
Due to the pronounced differences in the neutron scattering length density of different isotopes neutrons often provide better contrast and don't damage samples. On the other hand x-rays provide better Q resolution and higher Q values. In contrast to x-rays magnetic systems are easily probed by polarized neutron reflectometry due to magnetic dipole interaction with unpaired electrons.

Example of a Si/Pt monolayer

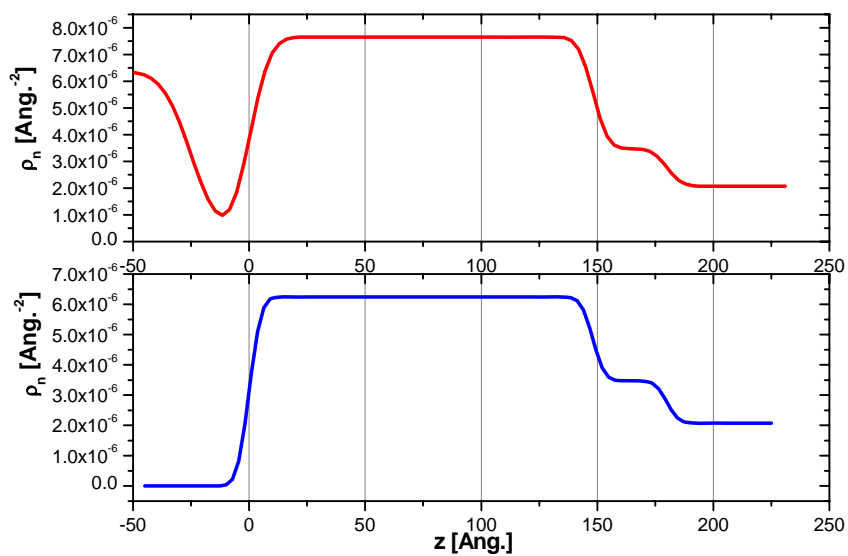
A nominal 15 nm thick layer of Pt has been magnetron sputtered on a Si(111) wafer and examined with x-ray and neutron reflectometry. The x-ray data are fitted with a single slab of Pt-layer of 16.05 nm thickness (grey curve) against air.



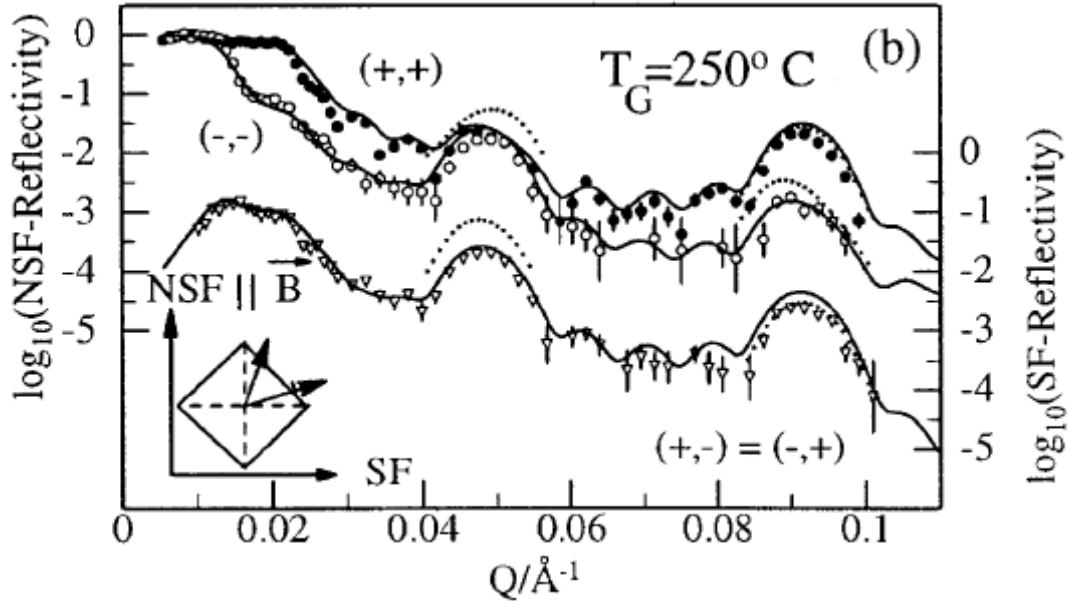
The neutron data show a two layer slab model with a Pt-layer of 14.80 nm and a SiO₂-layer underneath the Pt-layer of 3.18 nm thickness (red curve). The SiO₂ layer is not visible in the x-ray measurements due to the non-distinguishable x-ray scattering length density of Si of $2.012 \cdot 10^{-5} \text{ \AA}^{-2}$ and of SiO₂ of $2.015 \cdot 10^{-5} \text{ \AA}^{-2}$.



Measurement of the Pt-layer against liquid D₂O reveals the presence of an layer of organic material of 2.48 nm thickness which is not visible against air due to the neutron scattering length density of close to zero.



Polarised neutron reflectometry



G. Felcher et al., Physica B, 297 (2001) 87-93

The energy of a wave propagating in vacuum is

$$E_0 = \frac{\hbar^2}{2m} k_0^2$$

with $k_0 = 2\pi/\lambda$. On interaction with matter an interaction potential is added, which is described as a Fermi pseudo potential

$$V_F = \frac{\hbar^2}{2} 2\pi\rho b$$

Solving the Schroedinger equation for this interaction gives

$$\frac{\hbar^2}{2m} \frac{d^2 \varphi}{dr^2} + (E_0 - V_F) \varphi = 0$$

with $\varphi(r) = \varphi_+(r)|+\rangle + \varphi_-(r)|-\rangle$ for the two spin states of the neutron.

It follows with

$$k^2 = \frac{2m}{\hbar^2}(E_0 - V_F)$$

$$\frac{d^2\varphi}{dr^2} + k^2\varphi = 0$$

With $k^2 = n^2 k_0^2$ is

$$\frac{2m}{\hbar^2}(E_0 - V_F) = n^2 \frac{2m}{\hbar^2} E_0$$

$$n^2 = 1 - \frac{V_F}{E_0} = 1 - \frac{4\pi}{k_0^2} \rho b = 1 - \frac{\lambda^2}{\pi} \rho b$$

and

$$n \approx 1 - \frac{\lambda^2}{\pi} \rho b = 1 - \delta$$

If the interaction of the neutron wave is with a magnetic material the interaction potential is modified with a magnetic interaction by

$$V_M = V_F - g_n \mu_n \sigma B_{eff}$$

here, $B_{eff} = B_0 + \mu_0 M_{\parallel}$ with M_{\parallel} the magnetization parallel to the layer surface, B_0 the external magnetic field and $g_n \mu_n \sigma = \mu_m$ the neutron magnetic moment. This leads with $k^2 = n^2 k_0^2$ to

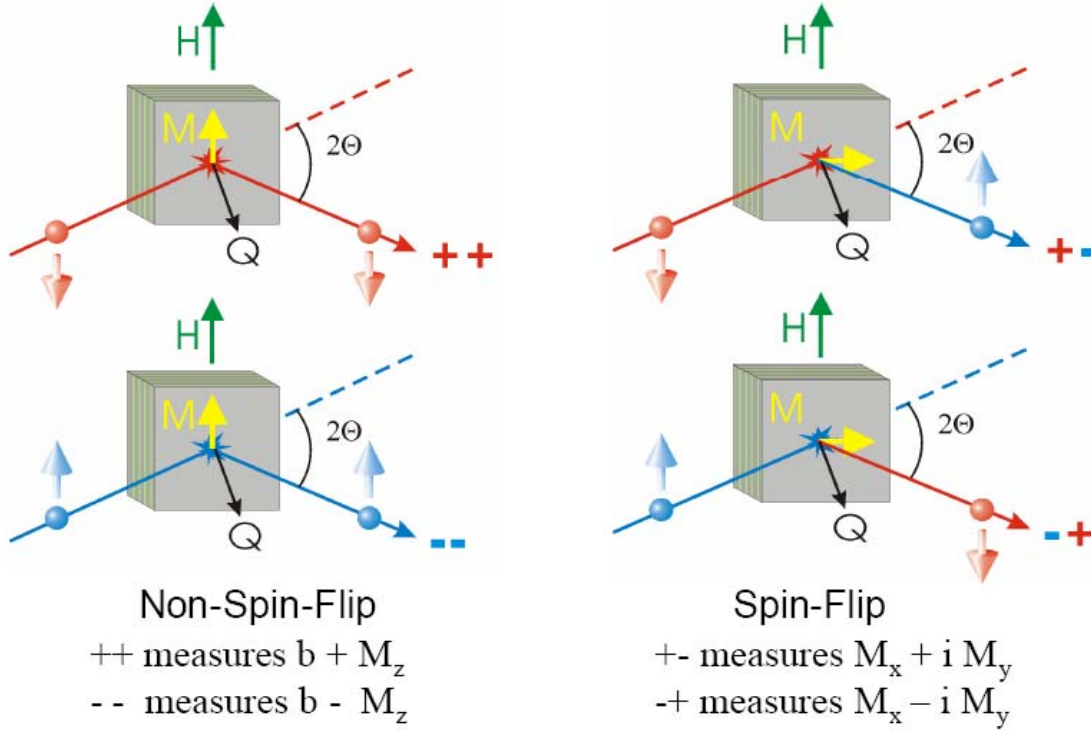
$$k_j^{\pm 2} = \frac{2m}{\hbar^2} E_0 - 4\pi \rho b_j \pm \frac{2m}{\hbar^2} g_n \mu_n |B_j|$$

which gives four wavevectors for the four spin states

$$k_j^{++2}, k_j^{+-2}, k_j^{-+2}, k_j^{--2}$$

and four reflectivities as

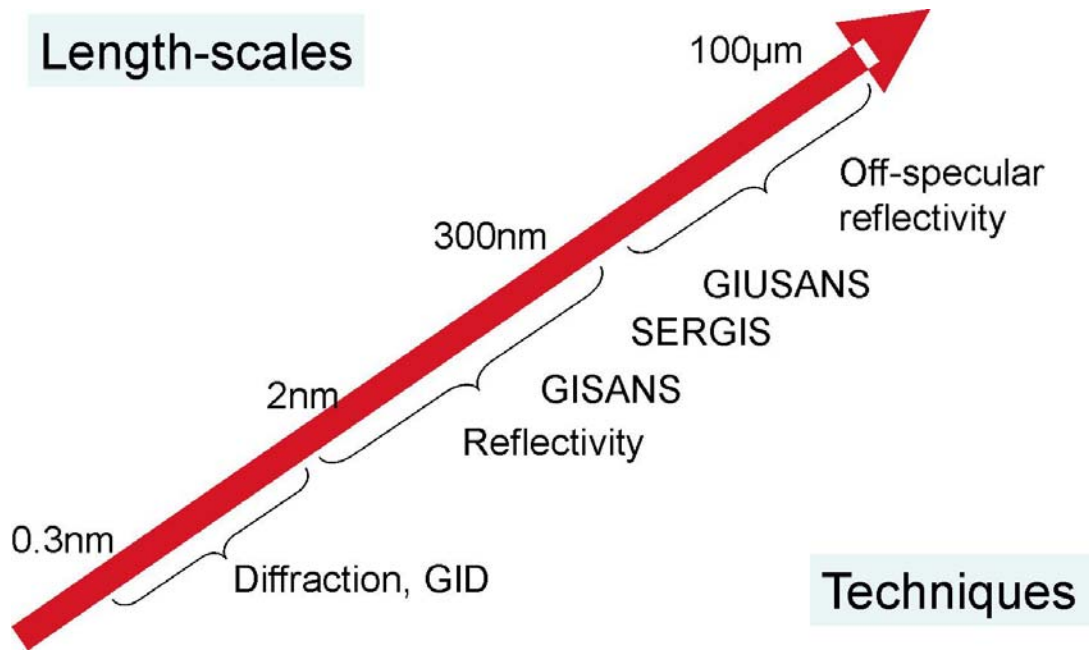
$$R^{++}, R^{+-}, R^{-+}, R^{--}$$



The reflectivity intensity for the ++ and +- spin state with external field \mathbf{B}_0 and magnetization \mathbf{M}_{\parallel} parallel to the plane now looks like

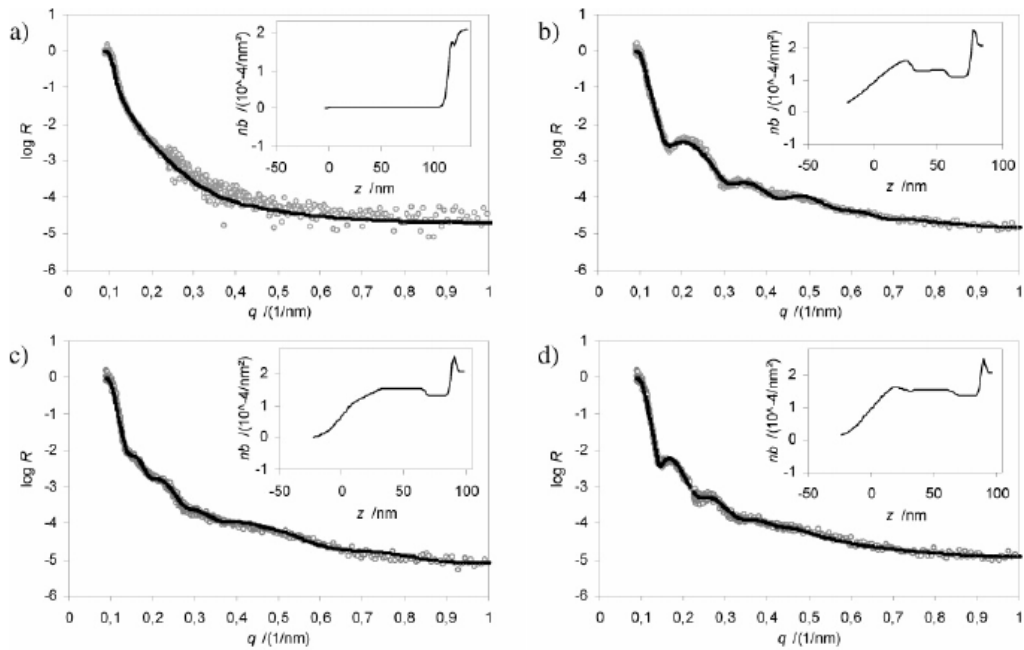
$$\begin{aligned}
 R^{++} &= |r^{++}|^2 \\
 &= \frac{\cos^2 \theta / 2 (q_{0,z} - q_{s,z}^+) (q_{0,z} + q_{s,z}^-) + \sin^2 \theta / 2 (q_{0,z} - q_{s,z}^-) (q_{0,z} + q_{s,z}^+)}{\cos^2 \theta / 2 (q_{0,z} + q_{s,z}^+) (q_{0,z} + q_{s,z}^-) + \sin^2 \theta / 2 (q_{0,z} + q_{s,z}^-) (q_{0,z} + q_{s,z}^+)} \\
 R^{+-} &= |r^{+-}|^2 \\
 &= \frac{2q_{0,z} \cos^2 \theta / 2 \sin^2 \theta / 2 (q_{s,z}^+ - q_{s,z}^-)}{\cos^2 \theta / 2 (q_{0,z} + q_{s,z}^+) (q_{0,z} + q_{s,z}^-) + \sin^2 \theta / 2 (q_{0,z} + q_{s,z}^-) (q_{0,z} + q_{s,z}^+)}
 \end{aligned}$$

The +- state is also called spin-flip state or orientation as the orientation of the outgoing neutron spin is flipped in comparison with the orientation of the incoming neutron spin. Similar expressions can be derived for other orientations of the magnetization.



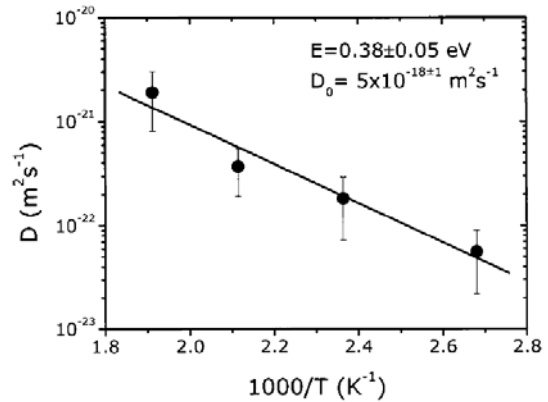
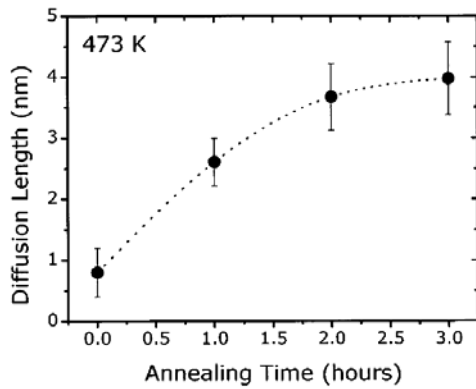
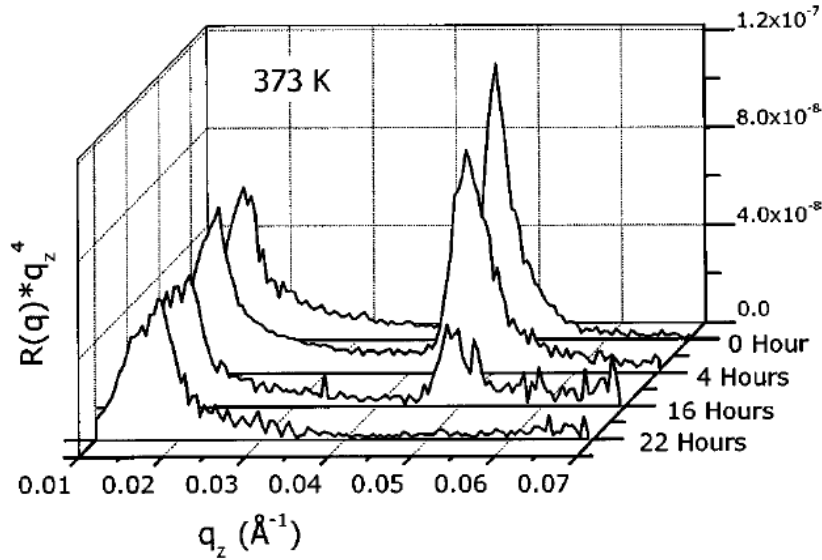
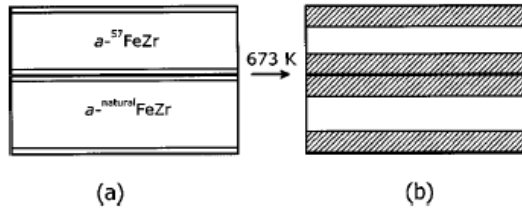
Reflectometry at solid/solid interfaces

- Transformation of Cross-Linked Poly(dimethylsiloxane) after Irradiation



[V. Graubner et al. Langmuir 21, 8940 (2005)]

- Iron self-diffusion in FeZr/⁵⁷FeZr multilayers



Decay of Bragg peak intensity in the neutron reflectivity pattern of $[\text{FeZr}/^{57}\text{FeZr}]_{20}$ isotopic multilayer after annealing and the diffusion length and Arrhenius behavior of the diffusivity.

[M. Gupta et al. PRB 70, 184206 (2004)]

- Nitrogen Diffusion in Amorphous Silicon Nitride Isotope Multilayers

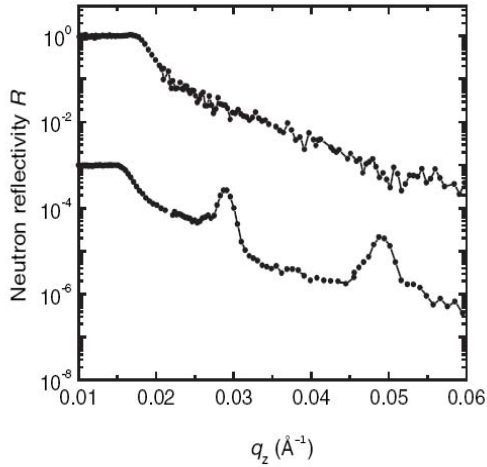


FIG. 1. Neutron reflectivity pattern of a $[\text{Si}_3^{14}\text{N}_4(19 \text{ nm})/\text{Si}_3^{15}\text{N}_4(6 \text{ nm})]_{20}$ isotopic multilayer (bottom) compared to the pattern of a not enriched Si_3N_4 film (top). The reflectivity pattern of the multilayer is divided by a factor of 1000 for clarity.

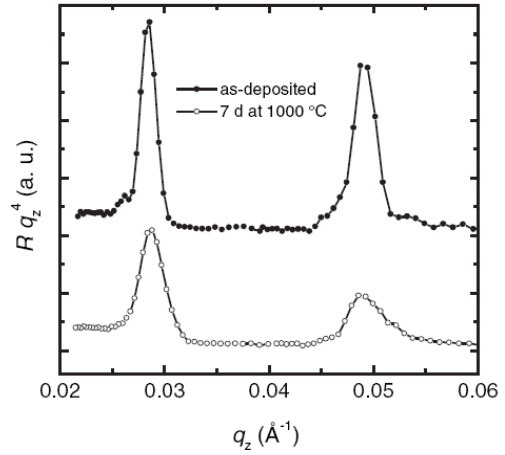


FIG. 2. Neutron reflectivity pattern of a $[\text{Si}_3^{14}\text{N}_4(19 \text{ nm})/\text{Si}_3^{15}\text{N}_4(6 \text{ nm})]_{20}$ isotopic multilayer in the as-deposited state (shifted for clarity) and after annealing for 7d at 1000°C . The patterns are multiplied by q_z^4 in order to correct for the background.

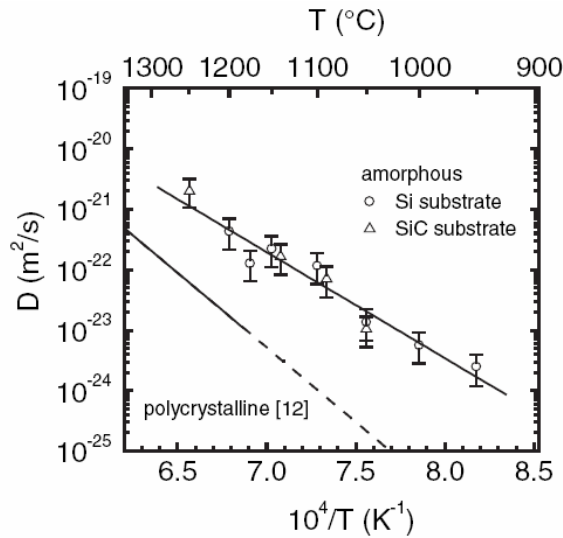
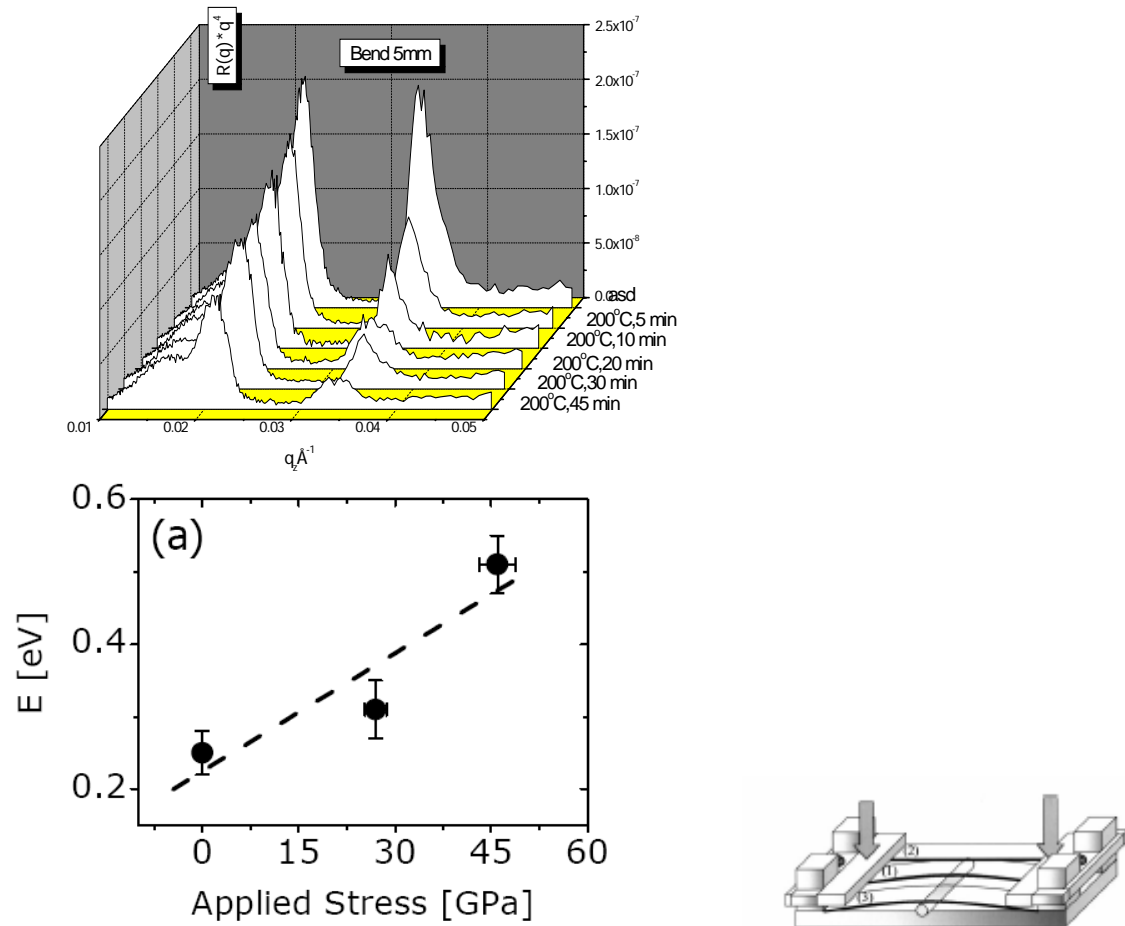


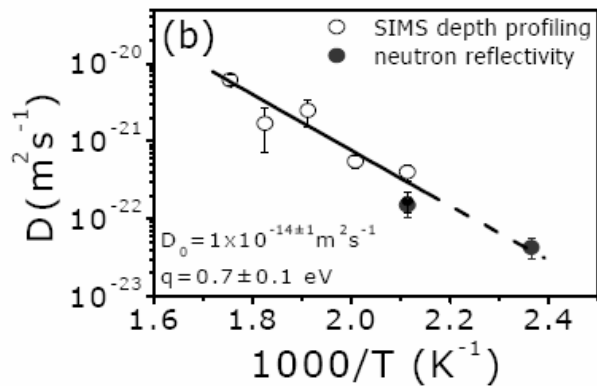
FIG. 3. Nitrogen diffusivities in amorphous Si_3N_4 films as a function of reciprocal temperature. The dashed line is an extrapolation of the experimental data on polycrystalline Si_3N_4 films represented by the solid line (after Ref. [12]).

[H. Schmidt et al., PRL 96, 055901 (2006)]

- Iron self-diffusion in FeZr/57FeZr multilayers

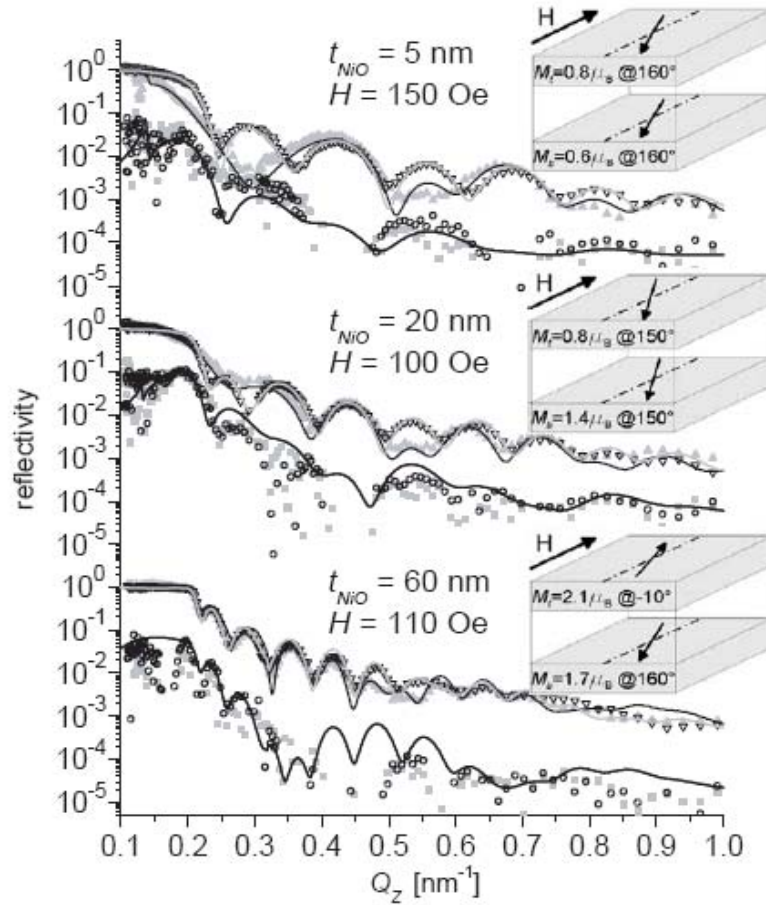


Variation of activation energy with the applied stress.



[M. Gupta et al., PSI Scientific Rep.2004, Vol., 68, M. Gupta et al. Defect Diff. Forum, 237-240 (2005), 548-553]

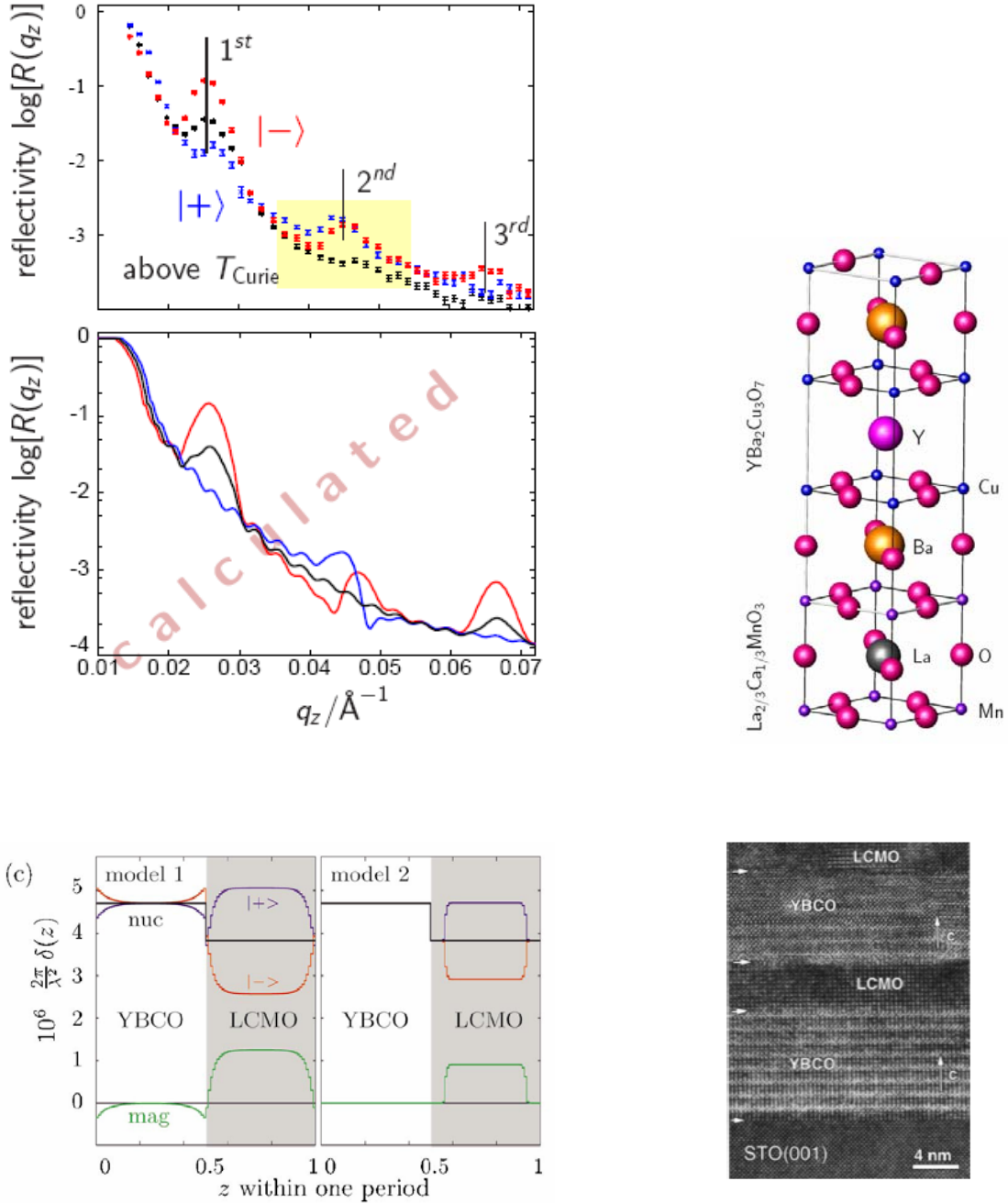
- Magnetic depth profiling of FM/AF/FM trilayers



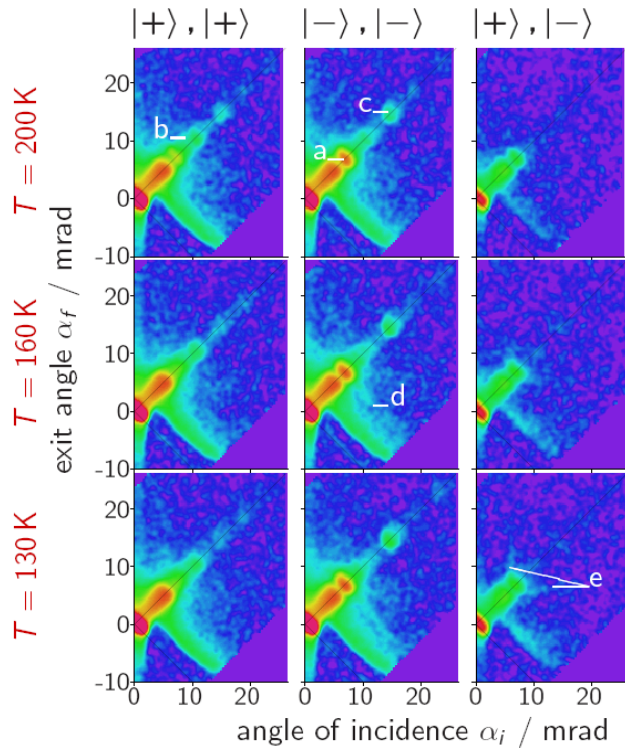
PNR of FeCoV/NiO (tNiO)/FeCoV trilayers measured at selected positions during the magnetization reversal. Experimental data are represented by Symbols, computed reflectivities are represented by lines. The insets show the average magnetization of individual FeCoV layers as obtained from modeling.

[C. Schanzer et al., Physica B 356, 2005, 46–50]

- Antiphase magnetic proximity effect in perovskite superconductor / ferromagnet multilayers



[J. Stahn et al., PRB **71**, 2005, 140509R]



No off-specular sheets at RT or 200 K
 \Rightarrow no structural roughness detectable

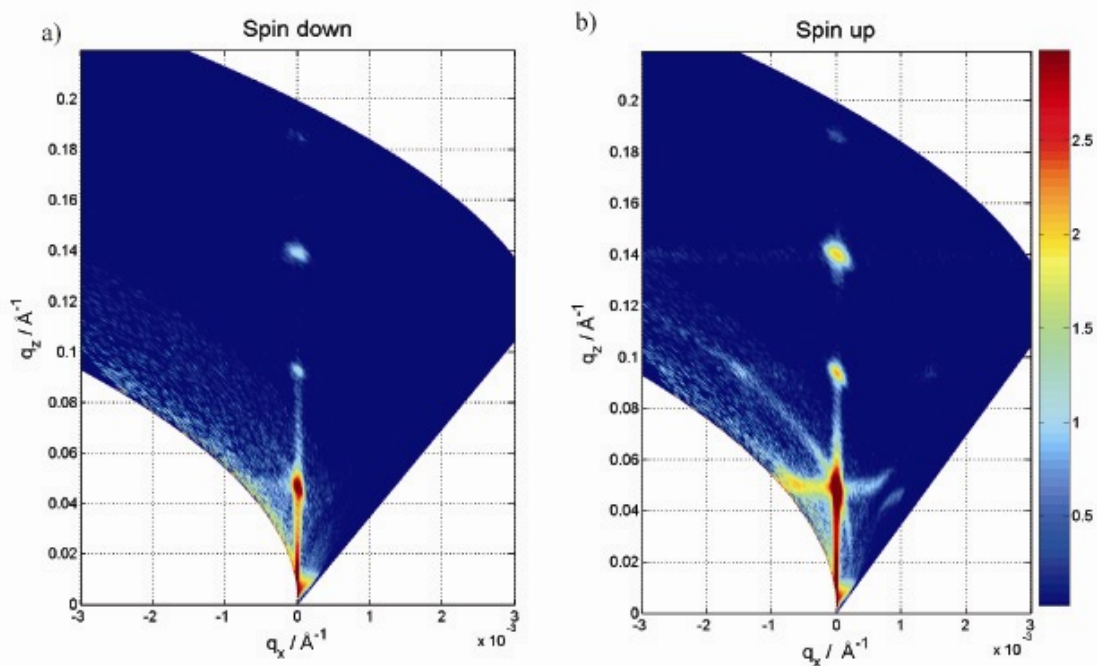
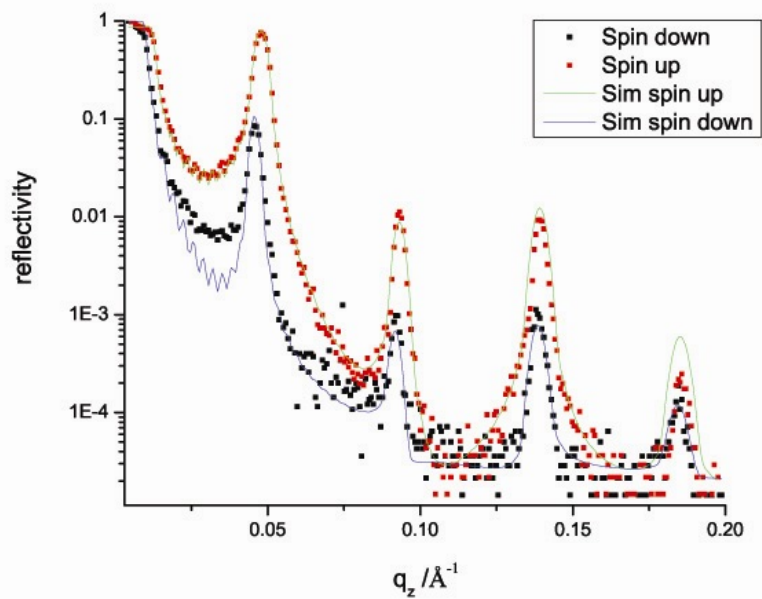
Increase of the Bragg sheet at 1st Bragg peak (d) below 160 K
 \Rightarrow magnetic roughness, correlated vertically

Appearance of sheets in the spin-flip channel (e)
 \Rightarrow magnetic moments not parallel to the neutron spins

Interpretation (of all measurements):
 Magnetic domains of similar size (≈ 5 to $10\mu\text{m}$) are formed in the LCMO layers. These are correlated through YBCO over the whole stack.

[J. Hoppler, Diploma Thesis]

- Polarised Neutron Reflectometry of Fe-Co-V Multilayers



Fe-Co-V/Ti bilayer, 15 bilayers with a repeat distance of 136 \AA
 [J. Padiyath, PhD Thesis, ETHZ, No. 16389, 2006].

- Resonant X-ray Reflectometry

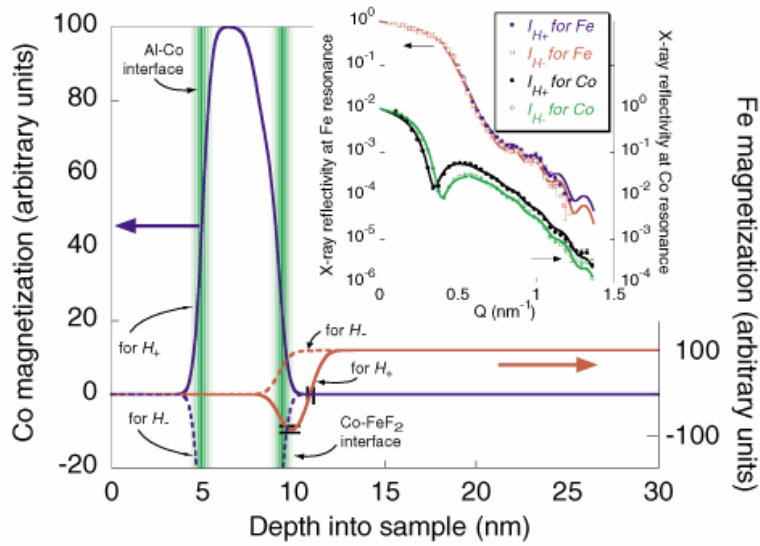


FIG. 2 (color). Spin density depth profiles for Co (blue) and Fe (red) spins obtained from the specular x-ray reflectivities (inset) at $H_{\pm} = \pm 796$ kA/m.

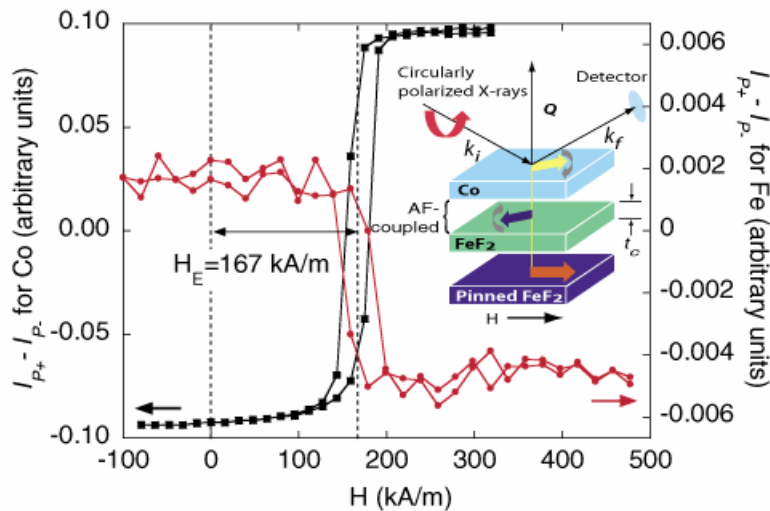
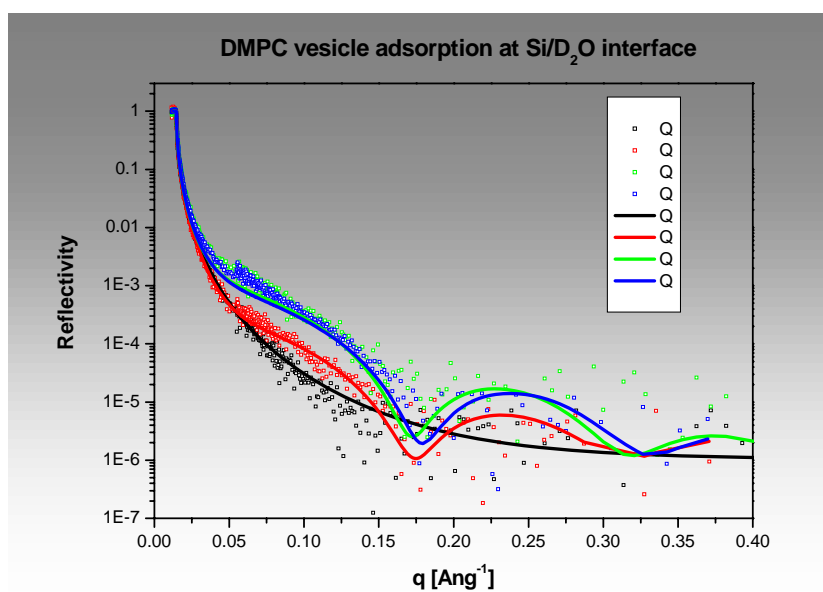
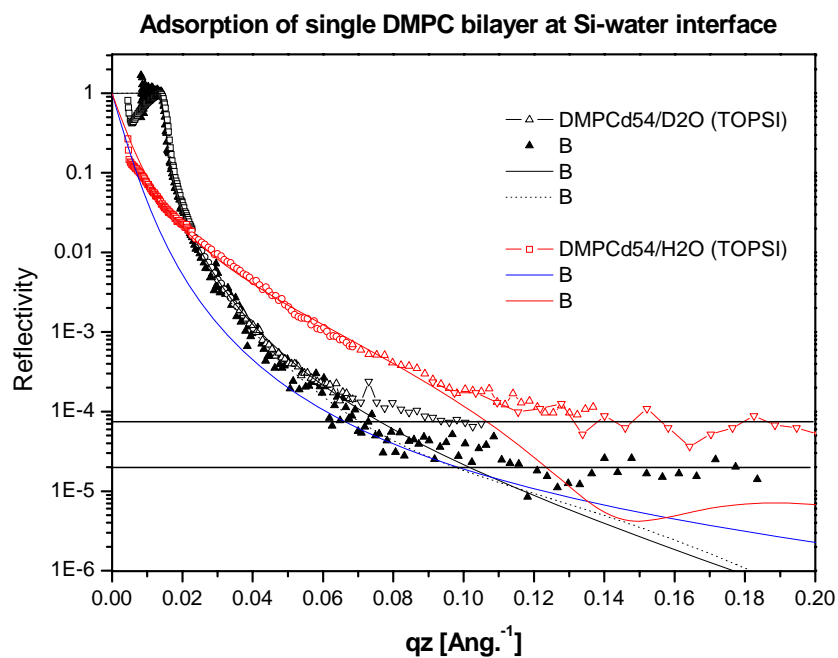


FIG. 1 (color). Hysteresis loops at $Q = 0.49$ and 0.38 nm $^{-1}$ for Co (■) and Fe (●), respectively. Inset: representations of the x-ray experiment and sample.

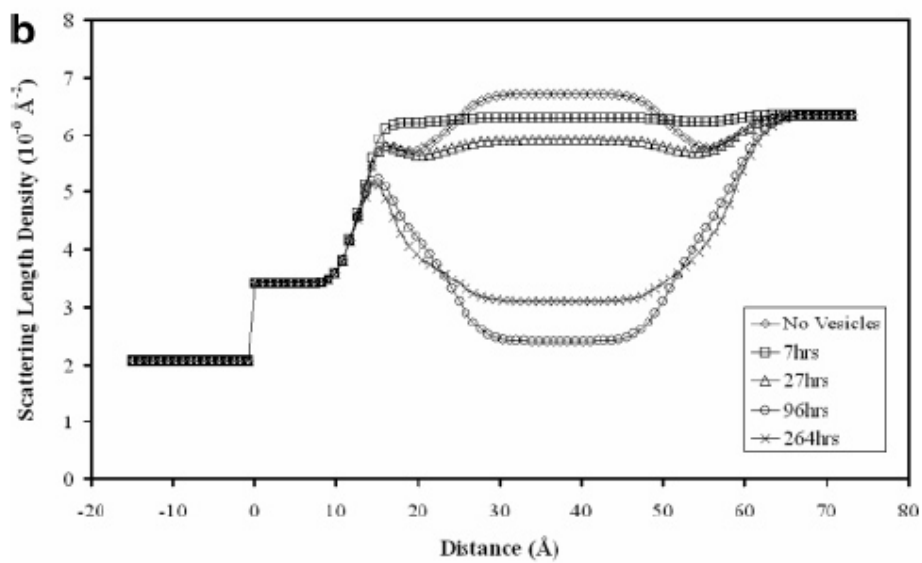
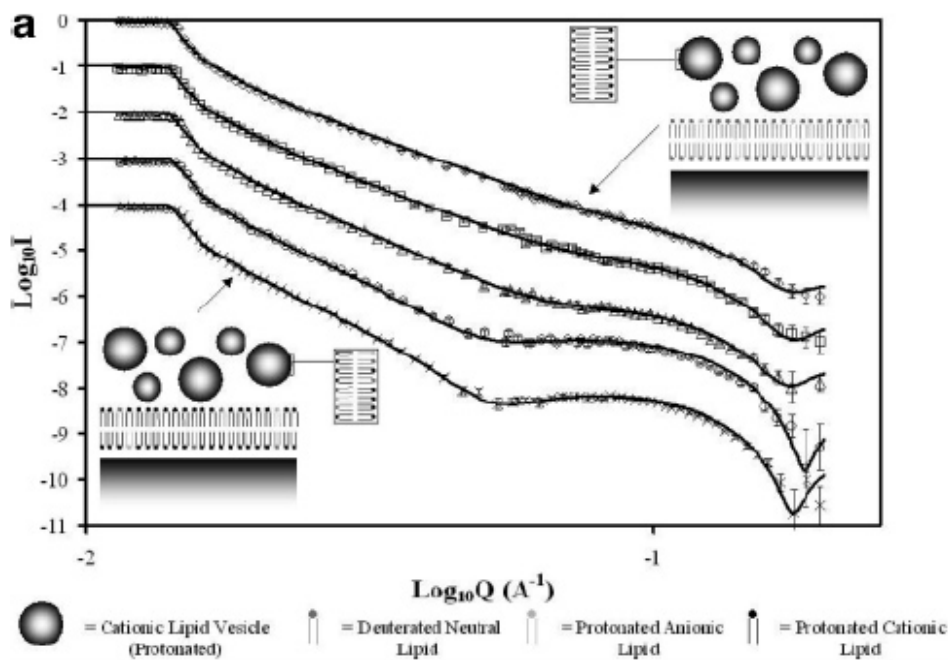
[Phys. Rev. Lett, 95, 2005, 047201]

Reflectometry at solid/liquid interfaces

- Neutron Reflectometry of Adsorbed Single Lipid Bilayer

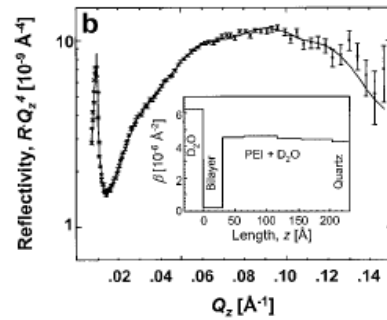
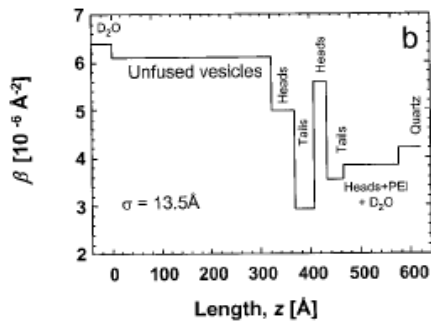
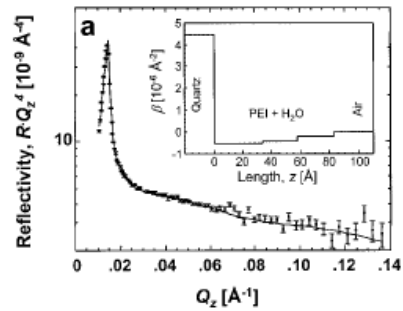
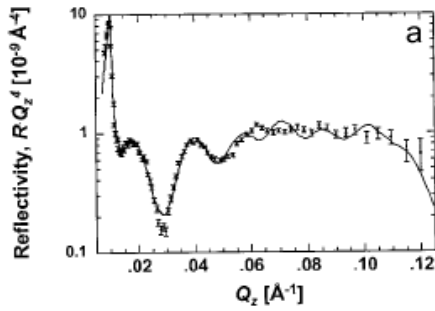
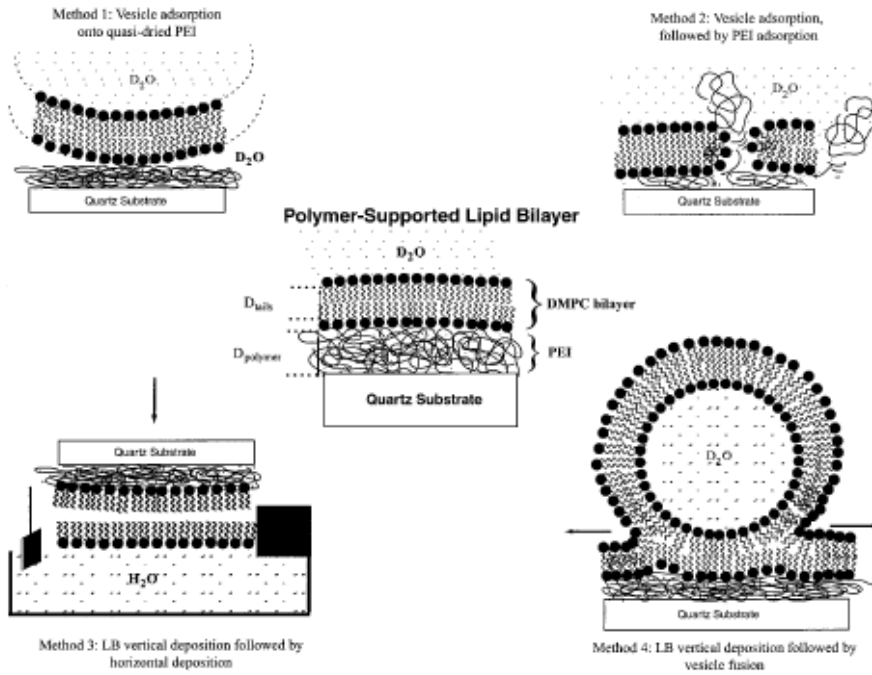


[T. Gutberlet et al., J. Phys.: Condens. Matter 16, 2004, S2469–S2476]

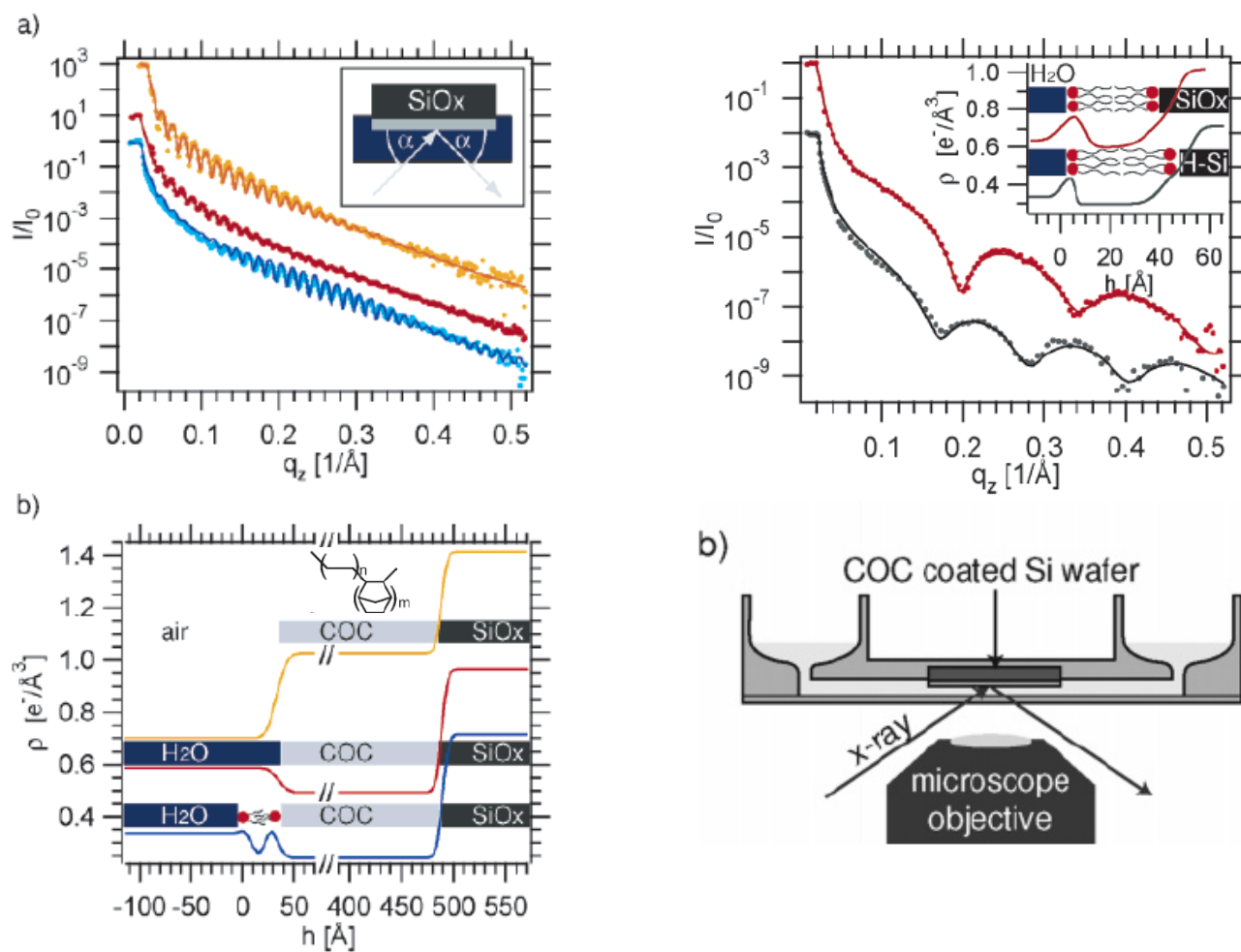


[P. Callow et.al., Langmuir, 2005, 21, 7912-7920]

- Polymer Adsorbed Phospholipid Layers

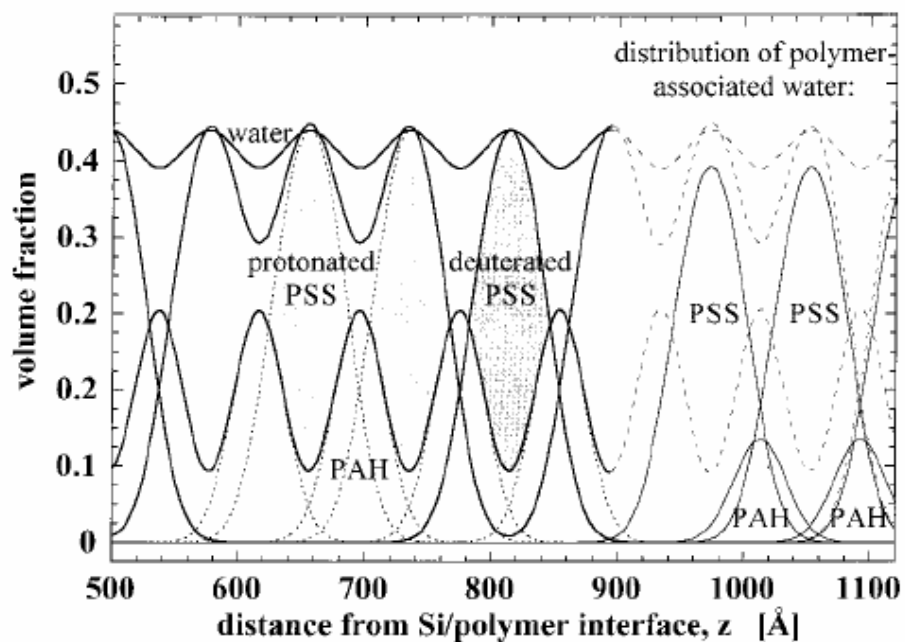
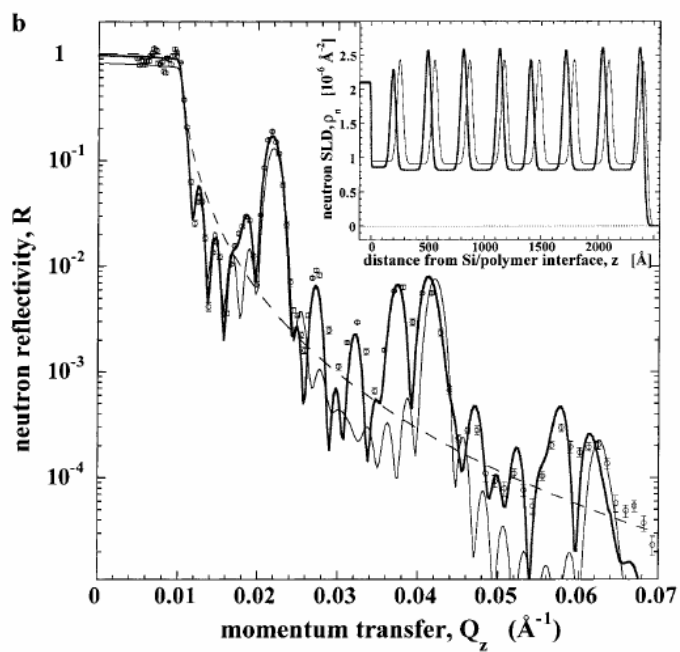


[J.Y. Wong et al, Biophys. J. 77, 1999, 1445]



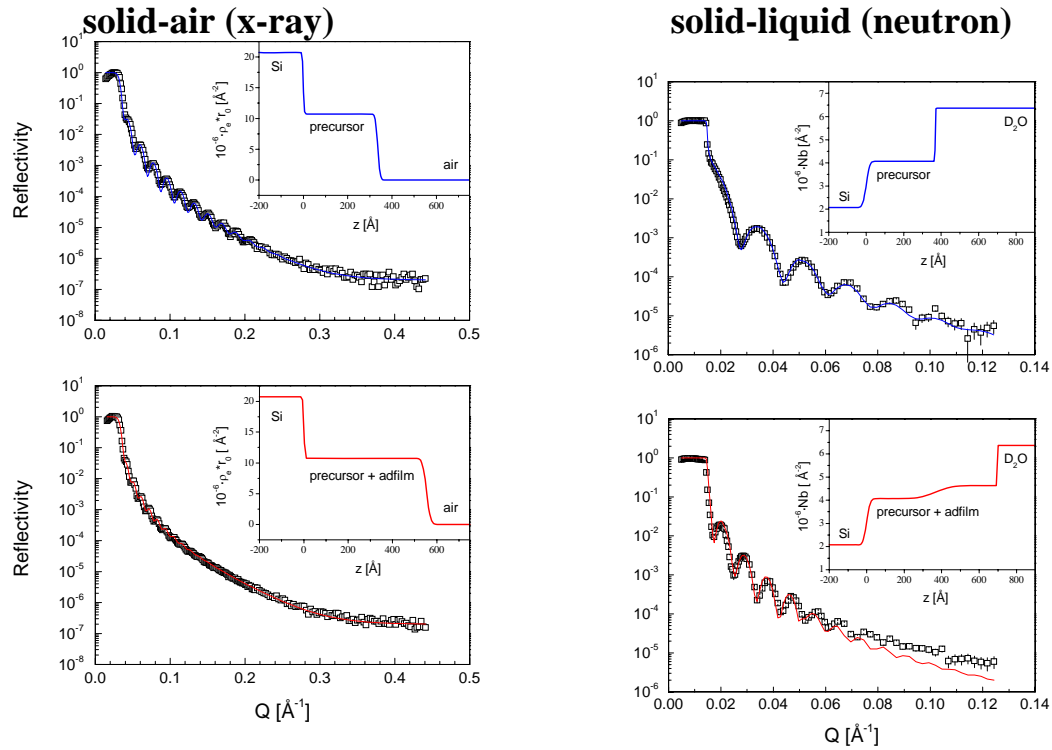
[M.B. Hochrein et al., Langmuir 2006, 22, 538-545]

- Polyelectrolyte cushions



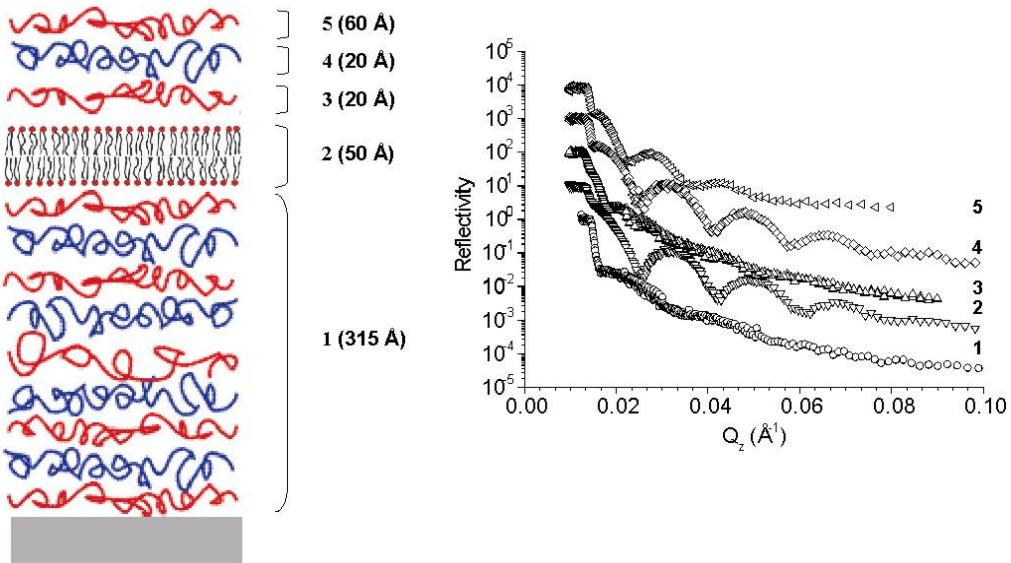
[M. Loesche et al., *Macromolecules* 1998, 31, 8893-8906]

- Swelling of a Polyelectrolyte Film



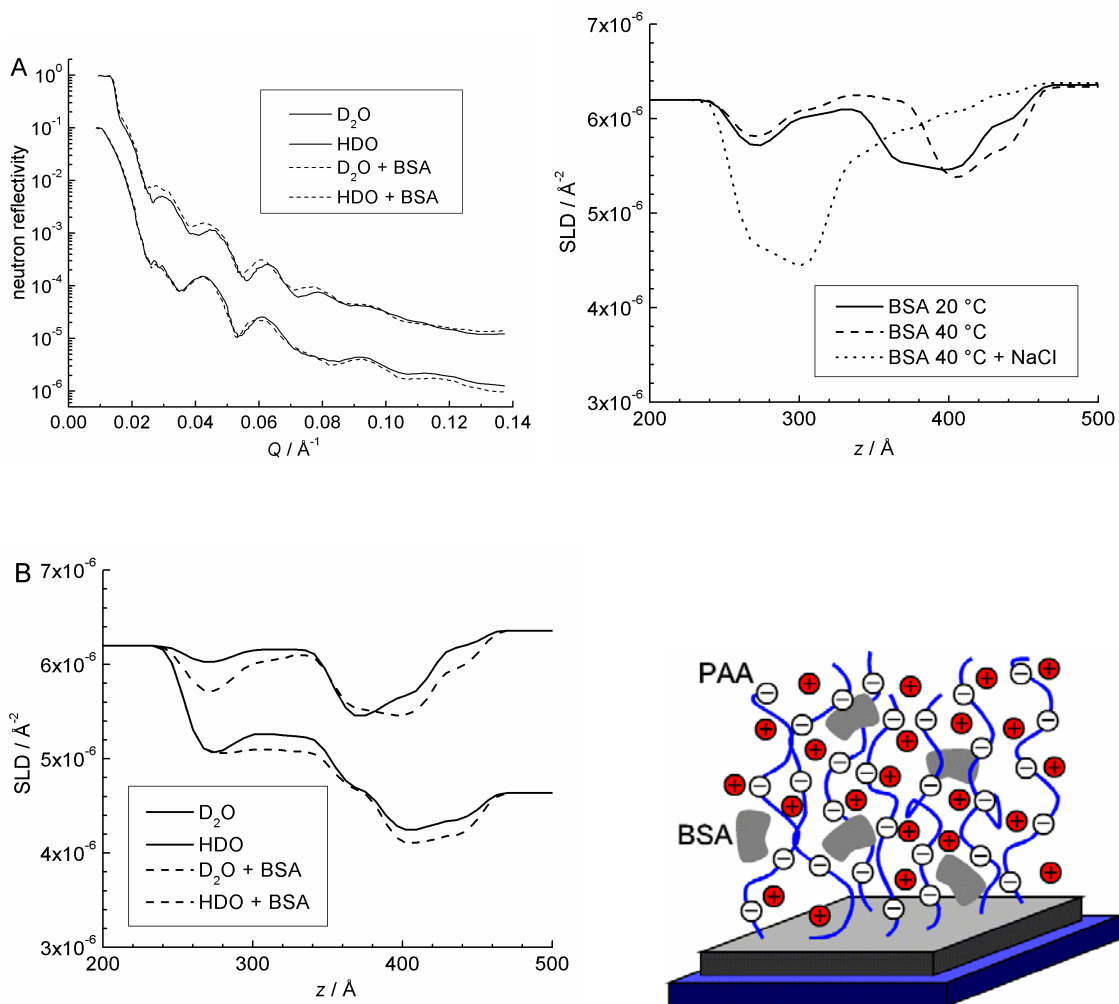
[R. Steitz et al., Colloids Surfaces A, 163, 2000, 63]

- Phospholipid Adsorption to Polyelectrolyte (PSS/PAH) Cushion



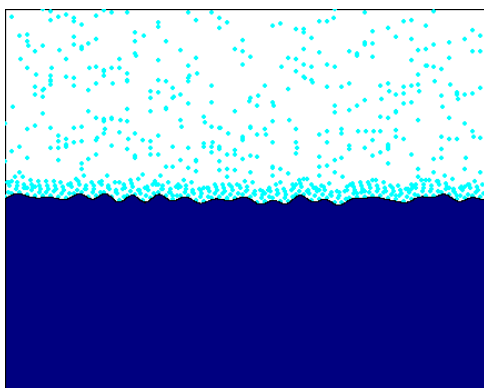
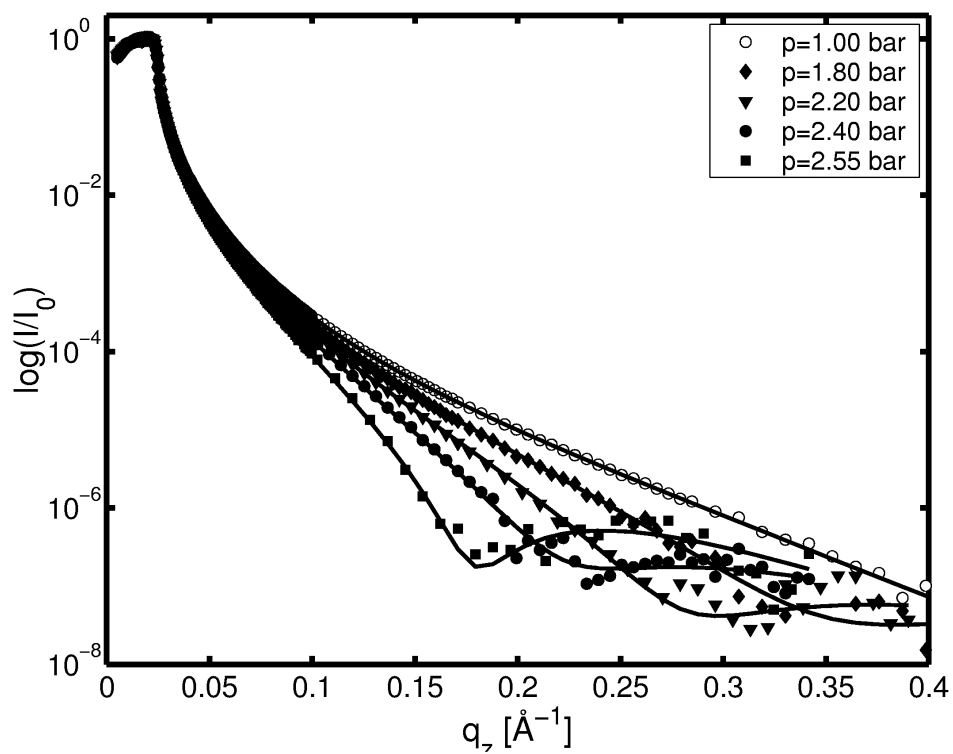
[C. Delajon et al., Langmuir, 21, 2005, 8509]

- Protein Binding Capacity of PAA Brushes



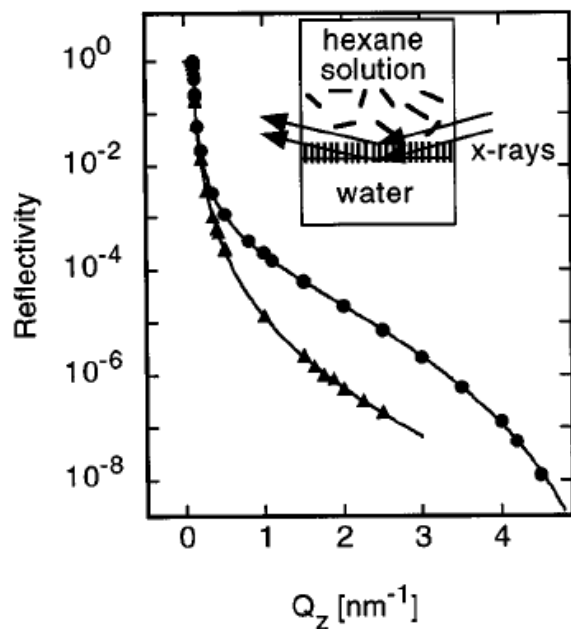
[C. Czeslik et al., Langmuir, submitted]

Reflectometry at liquid/liquid interfaces



X-ray reflectivity measurements of the isobutane-glycerol interface at 288K show an adsorption of liquid isobutane on the glycerol surface. The layer thickness and roughness increases with rising pressure.

[courtesy M.Paulus, Uni Dortmund]



[Z. Zhang et al, J. Phys Chem., 110, 1999, 7421]

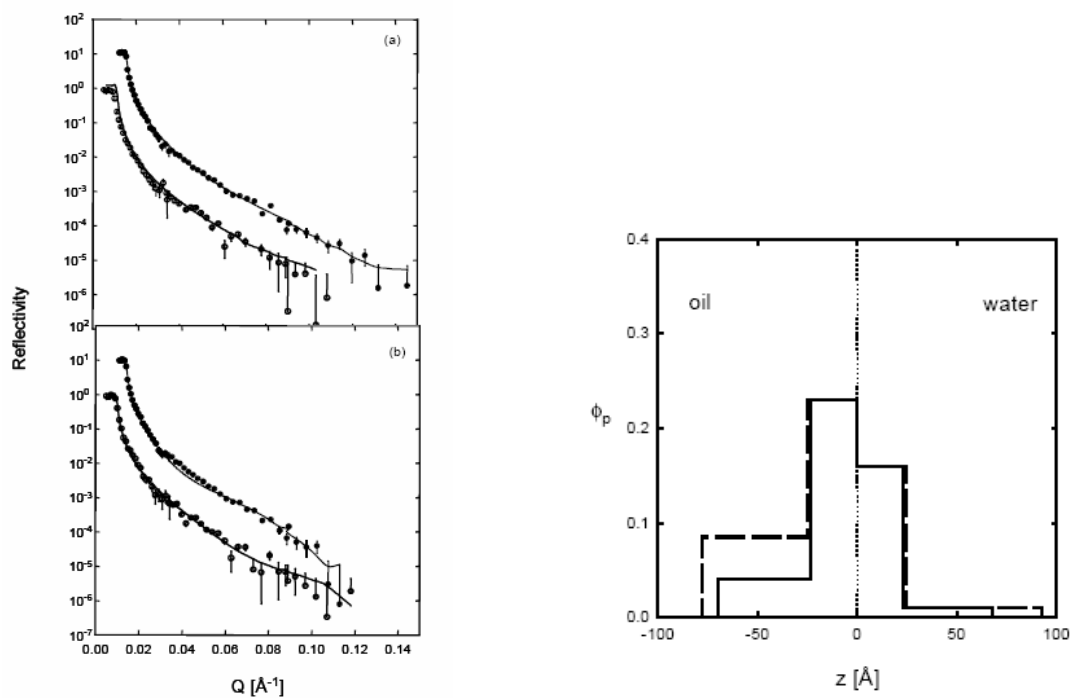
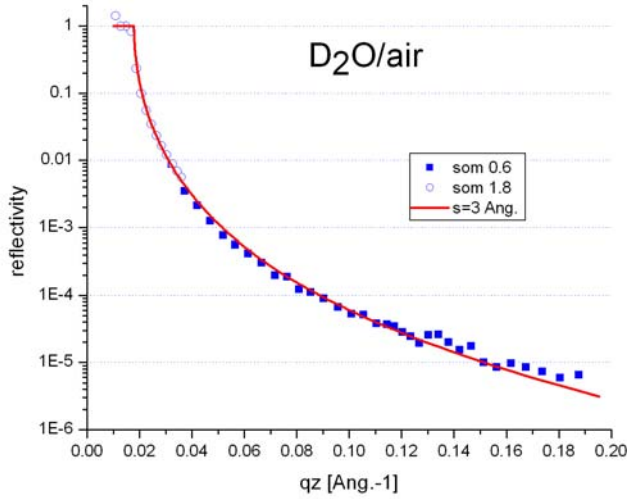


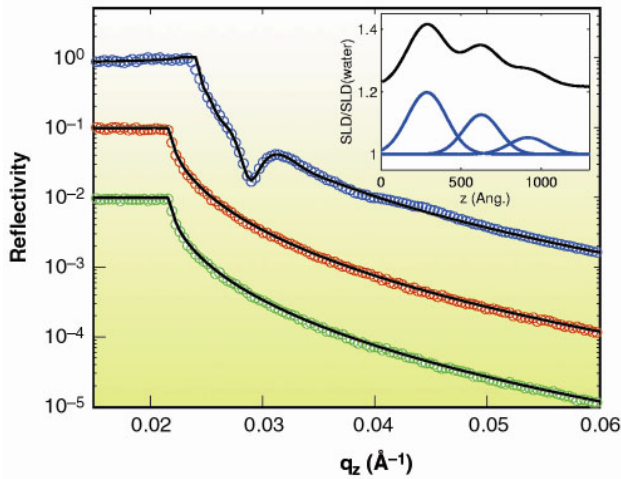
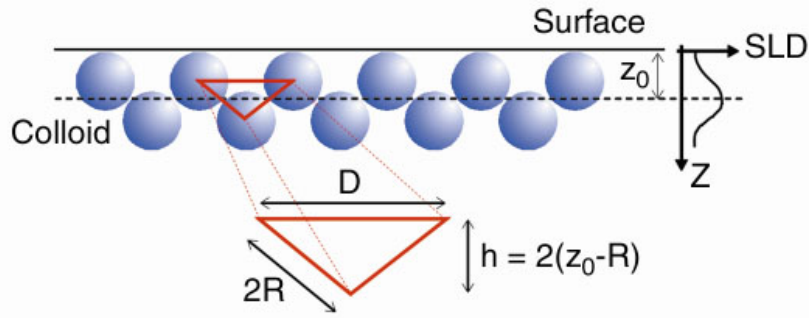
Figure 3. Reflectivity spectra for two different contrasts and spread amounts (Γ) and volume fraction profiles for PB-PEO copolymers spread at a hexadecane-water interface. (a) $\Gamma=4 \text{ mg m}^{-2}$, solid line on volume fraction profile; (b) $\Gamma=10 \text{ mg m}^{-2}$, dashed line.

[A. Zharbaksh et al., EPSRC Report, 2001]

Reflectometry at air/liquid interfaces



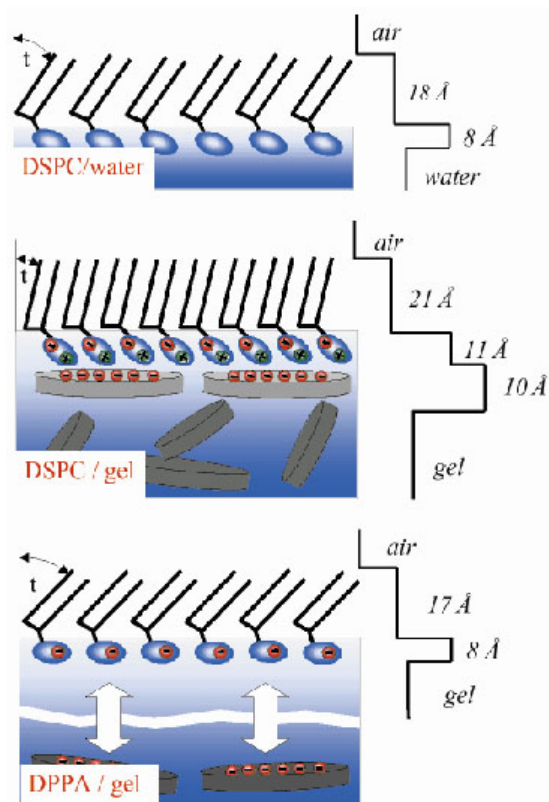
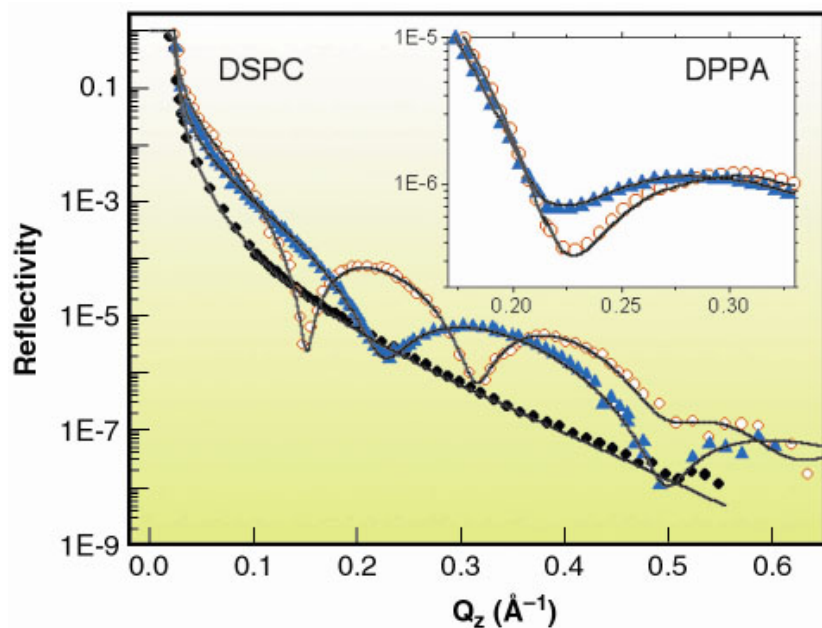
- Layering of Spherical Particles at Air/Water Interface



X-ray reflectivity profiles of the concentrated (blue) and dilute sample (red), and of the water solvent (green).

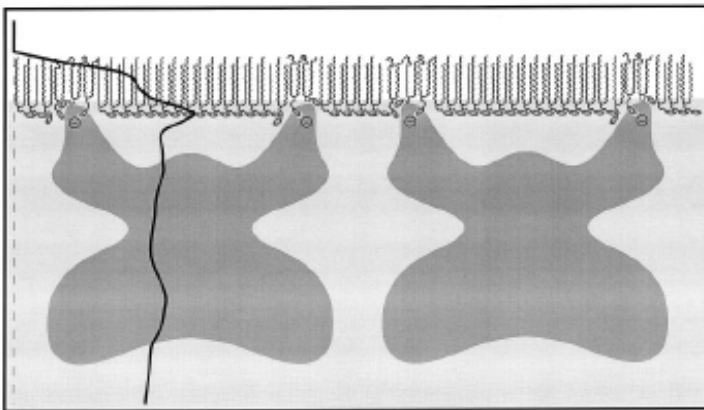
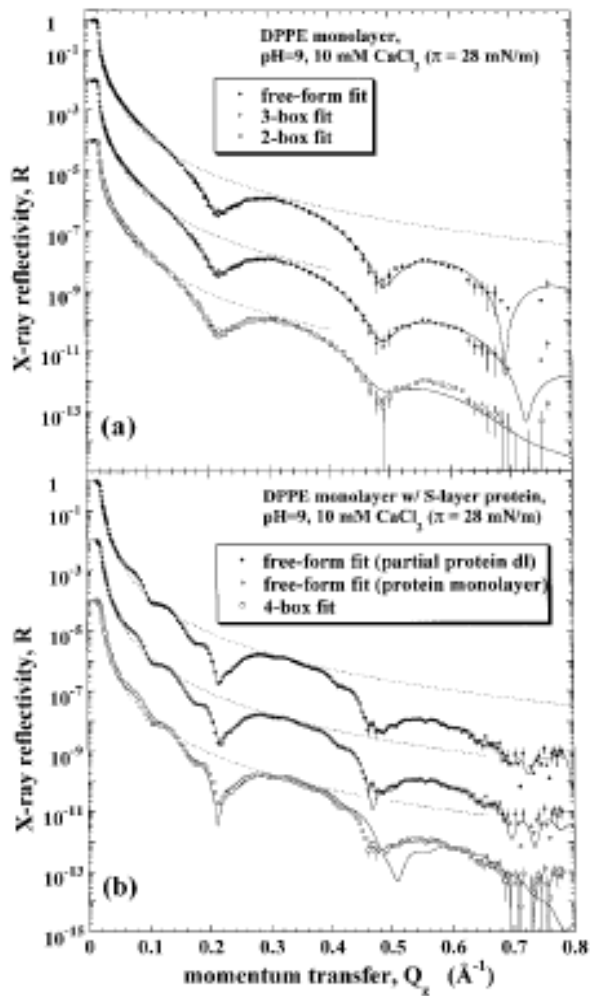
[A. Madsen et al., Phys. Rev. E., 64, 061406 (2001)]

- X-ray reflectivity of phospholipid monolayers on the surface of aqueous clay gels



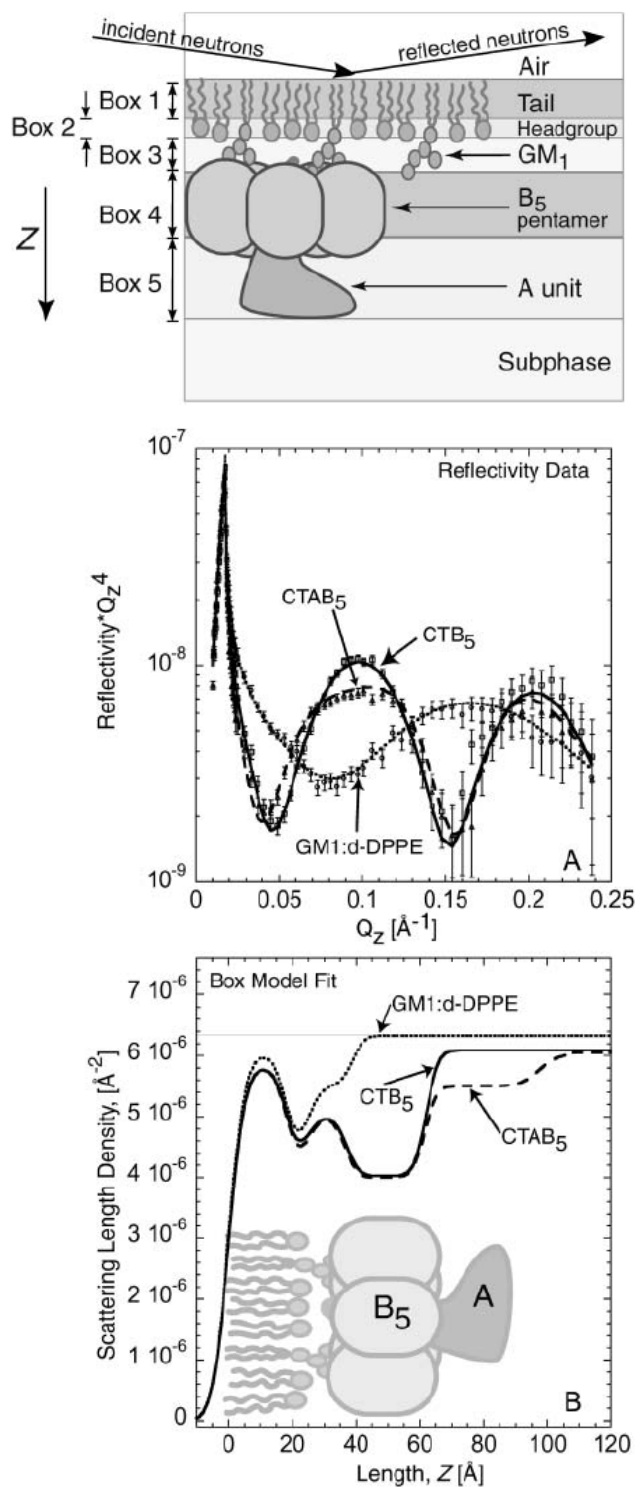
[B. Struth et al., Phys. Rev. Lett. 88, 025502 (2002)]

- S-layer protein coupling to a phospholipid monolayer



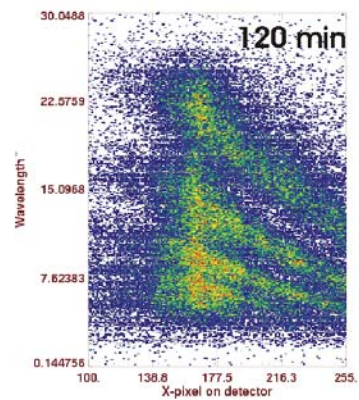
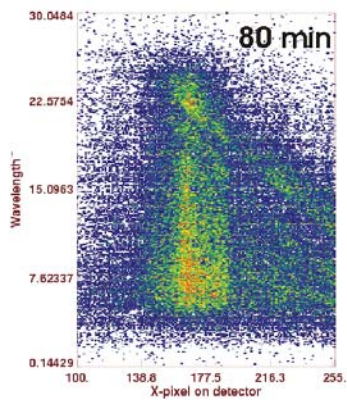
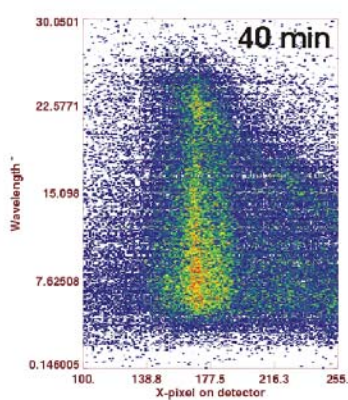
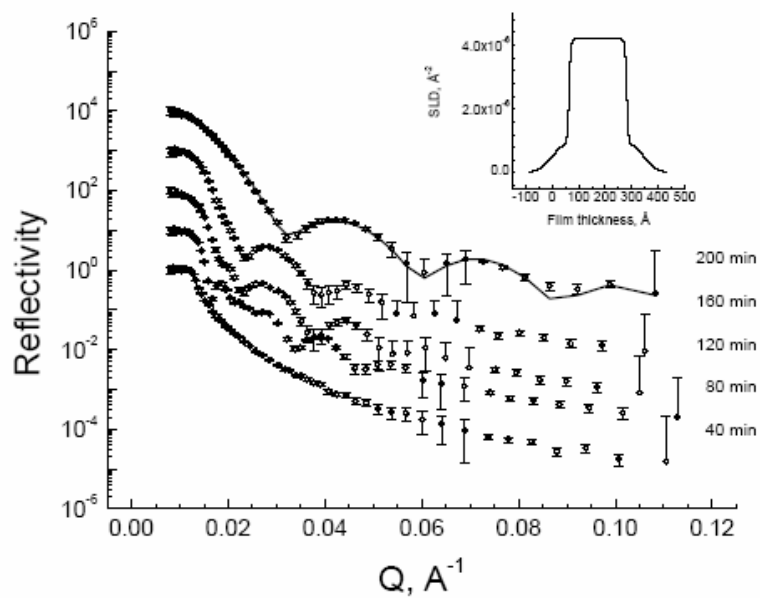
[M. Weygand et al., Biophys. J., 76, 1999, 458]

- Neutron Reflectivity of Cholera Toxin Assault on Lipid Monolayers



[C.E. Miller et al., Biophys. J., 86, 2004, 3700–3708]

- Formation of foam films

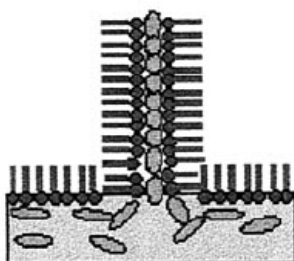


[R. Krastev et al., ILL Exp. Report, 9-10-744]

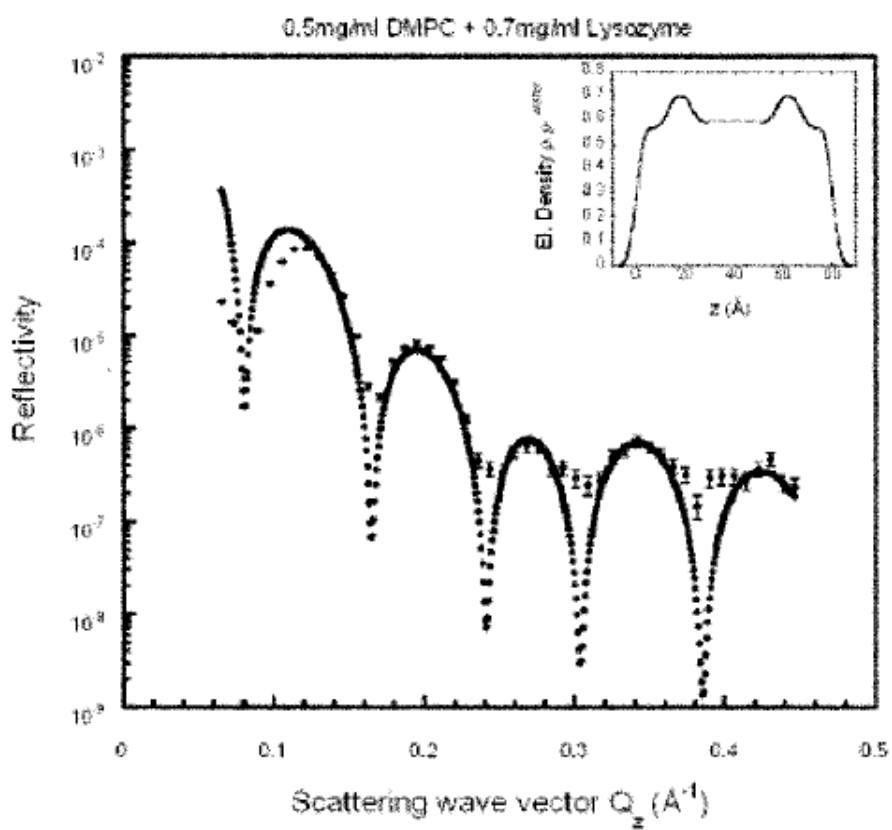
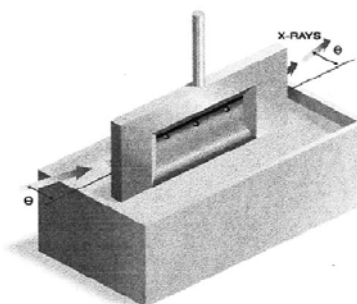
- Protein/Lipid Newton Black Film



(A)



(B)



[V. Petkova et al., Biophys. J., 82, 2002, 541–548]

References

- J. Als-Nielsen, D. McMorrow, *Elements of Modern X-ray Physics*, John Wiley & Sons, New York, 2001
- J. Daillant, A. Gibaud, *X-ray and Neutron Reflectivity: Principles and Applications*, Lecture Notes in Physics, Vol. 58, Springer Verlag, Berlin, 1999
- J. Penfoldt, R. K. Thomas, The application of the specular reflection of neutrons to the study of surfaces and interfaces, *J. Phys.: Condens. Matter*, 2, 1990, 1369-1412
- M. Tolan, W. Press, X-ray and neutron reflectivity, *Z. Kristallogr.*, 213, 1998, 319-336
- T.P. Russell, X-ray and neutron reflectivity for the investigation of polymers, *Mat. Sci. Rep.*, 5, 1990, 171-271
- C.F. Majkrzak, N.F. Berk, S. Krueger, U.A. Perez-Salas, *Structural Investigations of Membranes in Biology by Neutron Reflectometry*, in "Neutron Scattering in Biology", Eds. J. Fiter et.al., Springer, Berlin, 2006, pp. 237-278
- K. Stoev, K. Sakurai, Recent theoretical models in grazing incidence x-ray reflectometry, *Rigaku J.*, 14, 1997, 22-37
- H. Zabel, K. Theiss-Broehl, Polarized neutron reflectivity and scattering studies of magnetic heterostructures, *J.Phys. Cond. Mat.*, 15., 2003, S505-S517